Ministry for Primary Industries
Manatū Ahu Matua

The 2013 stock assessment of paua (*Haliotis iris*) for PAU 5B

New Zealand Fisheries Assessment Report 2014/45

D. Fu

ISSN 1179-5352 (online)
ISBN 978-0-478-43726-3 (online)

August 2014

New Zealand Government

Growing and Protecting New Zealand

Requests for further copies should be directed to:

Publications Logistics Officer
Ministry for Primary Industries
PO Box 2526
WELLINGTON 6140

Email: brand@mpi.govt.nz
Telephone: 0800 00 83 33
Facsimile: 04-894 0300

This publication is also available on the Ministry for Primary Industries websites at:
http://www.mpi.govt.nz/news-resources/publications.aspx
http://fs.fish.govt.nz go to Document library/Research reports

Contents

EXECUTIVE SUMMARY

Fu, D. (2014). The 2013 stock assessment of paua (*Haliotis iris*) for PAU 5B.

***New Zealand Fisheries Assessment Report 2014/45*. 51 p.**

This report summarises the stock assessment for PAU 5B which includes fishery data up to the 2012–13 fishing year. The report describes the model structure and output, including current and projected stock status. The stock assessment is implemented as a length-based Bayesian estimation model, with point estimates of parameters based on the mode of the joint posterior distribution, and uncertainty of model estimates investigated using the marginal posterior distributions generated from Markov chain-Monte Carlo simulation.

The data fitted in the assessment model were: (1) a standardised CPUE series based on the early CELR data, (2) a standardised CPUE series based on recent PCELR data, (3) commercial catch sampling length frequency series (CSLF), (4) tag-recapture length increment data, and (5) maturity-at-length data. The research diver survey data was not included in the base case because there is concern that the data is not a reliable index of abundance and the data is not representative of the whole PAU 5B stock.

The base case model (0.1) estimated that the spawning stock population in 2013 (B_{2013}) was about 44% (36–53%) of B_0. The model projection made for three years assuming current catch levels and using recruitments re-sampled from the recent model estimates, suggested that the spawning stock abundance will increase to about 48% (38–61%) of B_0 over the next three years. The projection also indicated that the probability of the spawning stock biomass being above the target (40% B_0) will increase from about 80% in 2013 to 93% in 2016, and that the stock status is very unlikely to be below the soft (20% B_0) and hard limits (10% B_0).

The assessment model indicated that the stock status was above target and the estimated stock abundance has been increasing over recent years, corroborating the observed trend in the fishery. Most data sets used in the model were collected from a wide range of areas and are believed to be representative of the stock. Results from sensitivity trials were close to the base case and they generally estimated optimistic stock status relative to the target. All runs considered in the assessment indicated that it was very unlikely the stock will fall below the soft or hard limits at current levels of catch.

1. INTRODUCTION

1.1 Overview

This report summarises the stock assessment for PAU 5B (Stewart Island, **Error! Reference source not found.**) with the inclusion of data to the end of 2012–13 fishing year. The report describes the model structure and output, including current and projected stock status. The stock assessment is conducted with the length-based Bayesian estimation model first used in 1999 for PAU 5B (Breen et al. 2000a) with revisions made for subsequent assessments in PAU 5B (Breen et al. 2000b, Breen & Smith 2008), PAU 4 (Breen & Kim 2004a), PAU 5A (Breen & Kim 2004b, Breen & Kim 2007, Fu & Mackenzie 2010a, b), PAU 5D (Breen et al. 2000a, Breen & Kim 2007, Fu 2013), and PAU 7 (Andrew et al. 2000, Breen et al. 2001, Breen & Kim 2003, 2005, McKenzie & Smith 2009, Fu 2012). PAU 5B was last assessed in 2007 (Breen & Smith 2008). The model was published by Breen et al. (2003).

The five sets of data used in the assessment were: (1) a standardised CPUE series covering 1990–2001 based on CELR data (CPUE), (2) a standardised CPUE series covering 2002–2013 based on PCELR data (PCPUE), (3) A commercial catch sampling length frequency series (CSLF), (4) tag-recapture length increment data, and (5) maturity-at-length data. Catch history was an input to the model, encompassing commercial, recreational, customary, and illegal catch. Another document describes the datasets that are used in the stock assessment and the updates that were made for the previous assessment (Fu et al. 2014).

There have been concerns over the research diver survey methodology and its usefulness in providing relative abundance indices (Cordue 2009, Haist 2010). In the most recent stock assessments of PAU 5D (Fu 2013) and PAU 7 (Fu 2011) the research diver survey indices (RDSI) and research diver survey length frequency (RDLF) data were not included in the base case. The same decision has been made here: the RDSI and RDLF were excluded from the base case but were included as a sensitivity trial.

The assessment was made in several steps. First, the model was fitted to the data with parameters estimated at the mode of their joint posterior distribution (MPD). Next, from the resulting fit, Markov chain-Monte Carlo (MCMC) simulations were made to obtain a large set of samples from the joint posterior distribution. From this set of samples, forward projections were made with a set of agreed indicators obtained. Sensitivity trials were explored by comparing MPD fits made with alternative model assumptions.

This document describes the model structure and assumptions, the fits to the data, estimates of parameters and indicators, and projection results. This report fulfils Objective 1 "Undertake a stock assessment for PAU 5B, using a length-based Bayesian model" of the Ministry for Primary Industries PAU201304.

1.2 Description of the fishery

The paua fishery was summarised by Schiel (1992), and in numerous previous assessment documents (e.g., Schiel 1989, McShane et al. 1994, 1996, Breen et al. 2000a, 2000b, 2001, Breen & Kim 2003, 2004a, 2004b, 2007). A summary of the PAU 5B fishery up to the 2012–13 fishing year is presented in Fu et al. (2014).

2. MODEL

This section gives an overview of the model used for the stock assessment of PAU 5B in 2013; for full description see Breen et al. (2003). The model was developed for use in PAU 5B in 1999 and has been revised each year for subsequent assessments, in many cases echoing changes made to the rock lobster assessment model (Kim et al. 2004), which is a similar but more complex length-based Bayesian model. The last revision made to the model was in 2012 for the assessment of PAU 5D (Fu 2013).

2.1 Changes to the 2007 assessment model of PAU 5B

One minor change was made to allow an annual step change in selectivity, echoing the gradual increase of minimum harvest size from 125 mm to 135 mm between 2006 and 2011:

$$V_k^{t,s} = \frac{1}{1+19^{-\left(\left(l_k - D_{50} - D_t^a D^s\right) / D_{95-50}\right)}} \quad \text{(See Section 2.2.11)}$$

In the 2010 assessment for PAU 5A, Fu & McKenzie (2010a, 2010b) reported B_{init}; the spawning stock biomass at the end of the initialisation phase (the equilibrium biomass assuming that recruitment is equal to base recruitment and with no fishing), and B_0; the equilibrium spawning stock biomass assuming that recruitment is equal to the average recruitment from the period for which recruitment deviations were estimated (B_0 normally differs from B_{init}). In this assessment a constraint was placed on the recruitment deviations so that their average is 1 for the period in which they are estimated, based on the parameterisation of Bull et al (2012). This ensures that the average recruitment for the period in which they are estimated (1980–2008) is close to R_0, and as a result B_{init} will be close to B_0.

2.2 Model description

The model partitioned the paua stock into a single sex population, with length classes from 70 mm to 170 mm, in groups of 2 mm (i.e., from 70 to under 72 mm, 72 mm to under 74 mm, etc.). The largest length bin is well above the maximum size observed. The stock was assumed to reside in a single, homogeneous area. The partition accounted for numbers of paua by length class within an annual cycle, where movement between length classes was determined by the growth parameters. Paua entered the partition following recruitment and were removed by natural mortality and fishing mortality.

The model annual cycle was based on the fishing year. Note that model references to "year" within this paper refer to the fishing year, and are labelled as the most recent calendar year, i.e., the fishing year 1998–99 is referred to as "1999" throughout. References to calendar years are denoted specifically.

The models were run for the years 1965–2013. The model assumes one time step within an annual cycle. Catches were collated for 1974–2013, and were assumed to increase linearly between 1965 and 1973 from 0 to the 1974 catch level. Catches included commercial, recreational, customary, and illegal catch, and all catches occurred at the same time step.

Recruitment was assumed to take place at the beginning of the annual cycle, and length at recruitment was defined by a uniform distribution with a range between 70 and 80 mm. Recruitment deviations were assumed known and equal to 1 for the years up to 1980. This was ten years before the length data were available (loosely based on the approximate time taken for recruited paua to appear at the right hand end of the length distribution). The stock-recruitment relationship is unknown for paua, but is likely to be weak (Shepherd et al. 2001). A relationship may exist on small scales, but may not be apparent when large-scale data are modelled (Breen et al. 2003). No explicit stock-recruitment relationship has been modelled in previous assessments. The Shellfish Working Group suggested assuming a Beverton-Holt stock-recruitment relationship with a steepness of 0.75 for the base case.

Maturity does not feature in the population partition. The model estimated proportions mature with the inclusion of length-at-maturity data. Growth and natural mortalities were also estimated within the model.

The models used two selectivities: the commercial fishing selectivity and research diver survey selectivity — both assumed to follow a logistic curve (see later) and then remain constant.

The model is implemented in AD Model Builder™ (Otter Research Ltd., http://otter-rsch.com/admodel.htm) version 9.0.65, compiled with the MinGW 4.50 compiler.

The seven sets of data fitted in the assessment model were: (1) a standardised CPUE series based on CELR data (2) a standardised CPUE series based on PCELR data (3) a standardised research diver survey index (RDSI) (4) a research diver survey proportions-at-lengths series (5) a commercial catch sampling length frequency series (6) tag-recapture length increment data and (7) maturity-at-length data (see Fu et al. 2014).

2.2.1 Estimated parameters

Parameters estimated by the model are as follows. The parameter vector is referred to collectively as θ.

$\ln(R0)$	natural logarithm of base recruitment
M	instantaneous rate of natural mortality
g_1	expected annual growth increment at length L_1
g_2	expected annual growth increment at length L_2
ϕ	CV of the expected growth increment
α	parameter that defines the variance as a function of growth increment
β	parameter that defines the variance as a function of growth increment
$\Delta_{\max}$	maximum growth increment
l_{50}^{g}	length at which the annual increment is half the maximum
l_{95}^{g}	length at which the annual increment is 95% of the maximum
l_{95-50}^{g}	difference between l_{50}^{g} and l_{95}^{g}
q^{I}	scalar between recruited biomass and CPUE
q^{I_2}	scalar between recruited biomass and PCPUE
q^{J}	scalar between numbers and the RDSI
L_{50}	length at which maturity is 50%
L_{95-50}	interval between L_{50} and L_{95}

T_{50}	length at which research diver selectivity is 50%
T_{95-50}	difference between T_{50} and T_{95}
D_{50}	length at which commercial diver selectivity is 50%
D_{95-50}	difference between D_{50} and D_{95}
D^{s}	step change in commercial diver selectivity
$\tilde{\sigma}$	common component of error
h	shape of CPUE *vs.* biomass relation
ε	vector of annual recruitment deviations, estimated from 1977 to 2013
H	steepness of the Beverton-Holt stock-recruitment relationship

2.2.2 Constants

l_k	length of a paua at the midpoint of the k^{th} length class (l_k for class 1 is 71 mm, for class 2 is 73 mm and so on)
σ_{MIN}	minimum standard deviation of the expected growth increment (assumed to be 1 mm)
σ_{obs}	standard deviation of the observation error around the growth increment (assumed to be 0.25 mm)
MLS_t	minimum legal size in year t (assumed to be 125 mm for all years)
$P_{k,t}$	a switch based on whether abalone in the k^{th} length class in year t are above the minimum legal size (MLS) ($P_{k,t}$ = 1) or below ($P_{k,t}$ = 0)
a,b	constants for the length-weight relation, taken from Schiel & Breen (1991) (2.592E-08 and 3.322 respectively, giving weight in kg)
w_k	the weight of an abalone at length l_k
ϖ^{I}	relative weight assigned to the CPUE dataset. This and the following relative weights were varied between runs to find a basecase with balanced residuals
ϖ^{I2}	relative weight assigned to the PCPUE dataset.
ϖ^{J}	relative weight assigned to the RDSI dataset
ϖ^{r}	relative weight assigned to RDLF dataset
ϖ^{s}	relative weight assigned to CSLF dataset
ϖ^{mat}	relative weight assigned to maturity-at-length data
ϖ^{tag}	relative weight assigned to tag-recapture data
κ_t^{s}	normalised square root of the number of paua measured greater than 113 mm in CSLF records for each year, normalised by the lowest year
κ_t^{r}	normalised square root of the number of paua measured greater than 89 mm in RDLF records for each year, normalised by the lowest year
$U^{\max}$	exploitation rate above which a limiting function was invoked (0.80 for the base case)
μ_M	mean of the prior distribution for M, based on a literature review by Shepherd & Breen (1992)
σ_M	assumed standard deviation of the prior distribution for M
σ_{ε}	assumed standard deviation of recruitment deviations in log space (part of the prior for recruitment deviations)

n_ε	number of recruitment deviations
L_1	length associated with g_1 (75 mm)
L_2	length associated with g_2 (120 mm)
D_t^a	Exogenous variable associated with the step change in commercial diver selectivity in year *t*

2.2.3 Observations

C_t	observed catch in year *t*
I_t	standardised CPUE in year *t*
$I2_t$	standardised PCPUE in year *t*
σ_t^I	standard deviation of the estimate of observed CPUE in year *t*, obtained from the standardisation model
cv_t^I	CV of the estimate of observed CPUE in year *t*, obtained from the standardisation model
σ_t^{I2}	standard deviation of the estimate of observed PCPUE in year *t*, obtained from the standardisation model
cv_t^{I2}	CV of the estimate of observed PCPUE in year *t*, obtained from the standardisation model
J_t	standardised RDSI in year *t*
σ_t^J	the standard deviation of the estimate of RDSI in year t, obtained from the standardisation model
cv_t^J	CV of the estimate of observed RDSI in year *t*, obtained from the standardisation model
$p_{k,t}^r$	observed proportion in the k^{th} length class in year *t* in RDLF
$p_{k,t}^s$	observed proportion in the k^{th} length class in year *t* in CSLF
l_j	initial length for the j^{th} tag-recapture record
d_j	observed length increment of the j^{th} tag-recapture record
Δt_j	time at liberty for the j^{th} tag-recapture record
p_k^{mat}	observed proportion mature in the k^{th} length class in the maturity dataset

2.2.4 Derived variables

$R0$	base number of annual recruits
$N_{k,t}$	number of paua in the k^{th} length class at the start of year *t*
$N_{k,t+0.5}$	number of paua in the k^{th} length class in the mid-season of year *t*
$R_{k,t}$	recruits to the model in the k^{th} length class in year *t*
g_k	expected annual growth increment for paua in the k^{th} length class
σ^{g_k}	standard deviation of the expected growth increment for paua in the k^{th} length class, used in calculating $\mathbf{G}$
$\mathbf{G}$	growth transition matrix

B_t	spawning stock biomass at the beginning of year t
$B_{t+0.5}$	spawning stock biomass in the mid-season of year t
B_0	equilibrium spawning stock biomass assuming no fishing and average recruitment from the period in which recruitment deviations were estimated.
B_{init}	spawning stock biomass at the end of initialisation phase (or B_{1964})
B_t^r	biomass of paua above the MLS at the beginning of year t
$B_{t+0.5}^r$	biomass of paua above the MLS in the mid-season of year t
B_0^r	equilibrium biomass of paua above the MLS assuming no fishing and average recruitment from the period in which recruitment deviations were estimated
B_{init}^r	biomass of paua above the MLS at the end of initialisation phase (or B_{1964}^r)
U_t	exploitation rate in year t
A_t	the complement of exploitation rate
$SF_{k,t}$	finite rate of survival from fishing for paua in the k^{th} length class in year t
V_k^r	relative selectivity of research divers for paua in the k^{th} length class
V_k^s	relative selectivity of commercial divers for paua in the k^{th} length class
$\sigma_{k,t}^r$	error of the predicted proportion in the k^{th} length class in year t in RDLF data
n_t^r	relative weight (effective sample size) of the RDLF data in year t
$\sigma_{k,t}^s$	error of the predicted proportion in the k^{th} length class in year t in CSLF data
n_t^s	relative weight (effective sample size)of the CSLF data in year t
σ_j^d	standard deviation of the predicted length increment for the j^{th} tag-recapture record
σ_j^{tag}	total error predicted for the j^{th} tag-recapture record
σ_k^{mat}	error of the proportion mature-at-length for the k^{th} length class
$-\ln(\mathbf{L})$	negative log-likelihood
f	total function value

2.2.5 Predictions

$\hat{I}_t$	predicted CPUE in year t
$\hat{I}2_t$	predicted PCPUE in year t
$\hat{J}_t$	predicted RDSI in year t
$\hat{p}_{k,t}^r$	predicted proportion in the k^{th} length class in year t in research diver surveys
$\hat{p}_{k,t}^s$	predicted proportion in the k^{th} length class in year t in commercial catch sampling
$\hat{d}_j$	predicted length increment of the j^{th} tag-recapture record
$\hat{p}_k^{mat}$	predicted proportion mature in the k^{th} length class

2.2.6 Initial conditions

The initial population is assumed to be in equilibrium with zero fishing mortality and the base recruitment. The model is run for 60 years with no fishing to obtain near-equilibrium in numbers-at-length. Recruitment is evenly divided among the first five length bins:

(1) $R_{k,t} = 0.2R0 \qquad \text{for } 1 \leq k \leq 5$

(2) $R_{k,t} = 0 \qquad \text{for } k > 5$

A growth transition matrix is calculated inside the model from the estimated growth parameters. If the growth model is linear, the expected annual growth increment for the k^{th} length class is:

(3) $$\Delta l_k = \left(\frac{L_2 g_1 - L_1 g_2}{g_1 - g_2} - l_k \right) \left[1 - \left(1 + \frac{g_1 - g_2}{L_1 - L_2} \right) \right]$$

The model uses the AD Model Builder™ function *posfun*, with a dummy penalty, to ensure a positive expected increment at all lengths, using a smooth differentiable function. The *posfun* function is also used with a real penalty to force the quantity $\left(1 + \frac{g_1 - g_2}{L_1 - L_2} \right)$ to remain positive. If the growth model is exponential (used for the base case), the expected annual growth increment for the k^{th} length class is:

(4) $$\Delta l_k = g_1 \left(g_2 / g_1 \right)^{(l_k - L_1)/(L_2 - L_1)}$$

again using posfun with a dummy penalty to ensure a positive expected increment at all lengths. If the inverse logistic growth model is used the expected annual growth increment for the k^{th} length class is:

(5) $$\Delta l_k = \frac{\Delta_{\max}}{\left(1 + \exp\left(\ln(19) \left(\left(l_k - l_{50}^g \right) / \left(l_{95}^g - l_{50}^g \right) \right) \right) \right)}$$

All the models were examined and the exponential growth model was chosen for fitting the tag-recapture data in the base case of the PAU 5B assessment.

The standard deviation of g_k is assumed to be proportional to g_k with minimum σ_{MIN}:

(6) $$\sigma^{g_k} = \left(g_k \phi - \sigma_{MIN} \right) \left(\frac{1}{\pi} \tan^{-1} \left(10^6 \left(g_k \phi - \sigma_{MIN} \right) \right) + 0.5 \right) + \sigma_{MIN}$$

Or a more complex functional form between the growth increment and its standard deviation can be defined as:

(7) $$\sigma^{g_k} = \left(\alpha (g_k)^{\beta} - \sigma_{MIN} \right) \left(\frac{1}{\pi} \tan^{-1} \left(10^6 \left(\alpha (g_k)^{\beta} - \sigma_{MIN} \right) \right) + 0.5 \right) + \sigma_{MIN}$$

From the expected increment and standard deviation for each length class, the probability distribution of growth increments for a paua of length l_k is calculated from the normal distribution and translated into the vector of probabilities of transition from the k^{th} length bin to other length bins to form the growth transition matrix **G**. Zero and negative growth increments are permitted, i.e., the probability of staying in the same bin or moving to a smaller bin can be non-zero.

In the initialisation, the vector $\mathbf{N_t}$ of numbers-at-length is determined from numbers in the previous year, survival from natural mortality, the growth transition matrix **G,** and the vector of recruitment $\mathbf{R_t}$:

(8) $$\mathbf{N_t} = \left(\mathbf{N_{t-1}}\, \mathrm{e}^{-M}\right) \bullet \mathbf{G} + \mathbf{R_t}$$

where the dot (•) denotes matrix multiplication.

2.2.7 Dynamics

2.2.7.1 Sequence of operations

After initialising, the first model year is 1965 and the model is run through to 2013. In the first nine years the model is run with an assumed catch vector, because it is unrealistic to assume that the fishery was in a virgin state when the first catch data became available in 1974. The assumed catch vector rises linearly from zero to the 1974 catch. These years can be thought of as an additional part of the initialisation, but they use the dynamics described in this section.

Model dynamics are sequenced as follows.

- Numbers at the beginning of year *t*-1 are subjected to fishing, then natural mortality, then growth to produce the numbers at the beginning of year *t*.
- Recruitment is added to the numbers at the beginning of year *t*.
- Biomass available to the fishery is calculated and, with catch, is used to calculate the exploitation rate, which is constrained if necessary.
- Half the exploitation rate (but no natural mortality) is applied to obtain mid-season numbers, from which the predicted abundance indices and proportions-at-length are calculated. Mid-season numbers are not used further.

2.2.7.2 Main dynamics

For each year *t*, the model calculates the start-of-the-year biomass available to the commercial fishery. Biomass available to the commercial fishery is:

(9) $$B_t = \sum_k N_{k,t} V_k^s w_k$$

(10) $$V_k^{t,s} = \frac{1}{1+19^{-\left(\left(l_k - D_{50}\right)/D_{95-50}\right)}} \qquad \text{for } t < 2007$$

(11) $$V_k^{t,s} = \frac{1}{1+19^{-\left(\left(l_k - D_{50} - D_t^a D^s\right)/D_{95-50}\right)}} \qquad \text{for } t \geq 2007$$

The observed catch is then used to calculate the exploitation rate, constrained for all values above U^{max} with the *posfun* function of AD Model Builder™. If the ratio of catch to available biomass exceeds U^{max}, then exploitation rate is constrained and a penalty is added to the total negative log-likelihood function. Let minimum survival rate A_{min} be 1-U^{max} and survival rate A_t be 1-U_t:

(12) $$A_t = 1 - \frac{C_t}{B_t} \qquad \text{for } \frac{C_t}{B_t} \le U^{\max}$$

(13) $$A_t = 0.5 A_{\min} \left[1 + \left(3 - \frac{2\left(1 - \frac{C_t}{B_t}\right)}{A_{\min}} \right)^{-1} \right] \qquad \text{for } \frac{C_t}{B_t} > U^{\max}$$

The penalty invoked when the exploitation rate exceeds U^{max} is:

(14) $$1000000\left(A_{\min} - \left(1 - \frac{C_t}{B_t}\right)\right)^2$$

This prevents the model from exploring parameter combinations that give unrealistically high exploitation rates. Survival from fishing is calculated as:

(15) $$SF_{k,t} = 1 - (1 - A_t) P_{k,t}$$

or

(16) $$SF_{k,t} = 1 - (1 - A_t) V_k^s$$

The vector of numbers-at-length in year t is calculated from numbers in the previous year:

(17) $$\mathbf{N_t} = \left(\left(\mathbf{SF_{t-1}} \otimes \mathbf{N_{t-1}} \right) e^{-M} \right) \bullet \mathbf{G} + \mathbf{R_t}$$

where $\otimes$ denotes the element-by-element vector product. The vector of recruitment, $\mathbf{R_t}$, is determined from *R0*, estimated recruitment deviations, and the stock-recruitment relationship:

(18) $$R_{k,t} = 0.2 R0 e^{\left(\varepsilon_t - 0.5\sigma_t^2\right)} \frac{B_{t-1+0.5}}{B_0} / \left(1 - \frac{5H-1}{4H} \left(1 - \frac{B_{t-1+0.5}}{B_0} \right) \right) \qquad \text{for } 1 \le k \le 5$$

(19) $$R_{k,t} = 0 \qquad \text{for } k > 5$$

The recruitment deviation parameters ε_t were estimated for all years from 1980. The recruitment deviations were constrained to have a mean of 1 in arithmetic space.

The model predicts CPUE in year t from mid-season recruited biomass, the scaling coefficient, and the shape parameter:

(20) $$\hat{I}_t = q^I \left(B_{t+0.5} \right)^h$$

Available biomass $B_{t+0.5}$ is the mid-season vulnerable biomass after half the catch has been removed (no natural mortality is applied, because the time over which half the catch is removed might be short). It is calculated as in equation (9), but using the mid-year numbers, $N_{k,t+0.5}$:

(21) $$N_{k,t+0.5}^{vuln} = N_{k,t}\left(1-\frac{(1-A_t)}{2}V_k^s\right).$$

Similarly,

(22) $$\hat{I}2_t = q^{I2}\left(B_{t+0.5}\right)^h = Xq^I\left(B_{t+0.5}\right)^h$$

The same shape parameter *h* is used for both the early and recent CPUE series: experimentation outside the model showed that this was appropriate despite the different units of measurement for the two series. The predicted research diver survey index is calculated from mid-season model numbers in bins greater than 89 mm length, taking into account research diver selectivity-at-length:

(23) $$N_{k,t+0.5}^{res} = N_{k,t}\left(1-\frac{(1-A_t)}{2}V_k^r\right)$$

(24) $$\hat{J}_t = q^J\sum_{k=11}^{55} N_{k,t+0.5}^{res}$$

where the scalar is estimated and the research diver selectivity V_k^r is calculated from:

(25) $$V_k^r = \frac{1}{1+19^{-\left((l_k-T_{50})/T_{95-50}\right)}}$$

The model predicts proportions-at-length for the RDLF from numbers in each length class for lengths greater than 89 mm:

(26) $$\hat{p}_{k,t}^r = \frac{N_{k,t+0.5}^{res}}{\sum_{k=11}^{51} N_{k,t+0.5}^{res}} \qquad \text{for } 11 \le k < 51$$

Predicted proportions-at-length for CSLF are similar:

(27) $$\hat{p}_{k,t}^s = \frac{N_{k,t+0.5}^{vuln}}{\sum_{k=23}^{51} N_{k,t+0.5}^{vuln}} \qquad \text{for } 23 \le k < 51$$

The predicted increment for the j^{th} tag-recapture record, using the linear model, is:

(28) $$\hat{d}_j = \left(\frac{\beta g_\alpha - \alpha g_\beta}{g_\alpha - g_\beta} - L_j\right)\left[1 - \left(1 + \frac{g_\alpha - g_\beta}{\alpha - \beta}\right)^{\Delta t_j}\right]$$

where Δt_j is in years. For the exponential model (used in the base case) the expected increment is

(29) $$\hat{d}_j = \Delta t_j g_\alpha \left(g_\beta / g_\alpha\right)^{(L_j - \alpha)/(\beta - \alpha)}$$

The error around an expected increment is:

(30) $$\sigma_j{}^d = \left(\hat{d}_j\phi - \sigma_{MIN}\right)\left(\frac{1}{\pi}\tan^{-1}\left(10^6\left(\hat{d}_j\phi - \sigma_{MIN}\right)\right) + 0.5\right) + \sigma_{MIN}$$

Predicted maturity-at-length is:

(31) $$\hat{p}_k^{mat} = \frac{1}{1 + 19^{-\left((l_k - L_{50})/L_{95-50}\right)}}$$

2.2.8 Fitting

2.2.8.1 Likelihoods

The distribution of CPUE is assumed to be normal-log and the negative log-likelihood is:

(32) $$-\ln(\mathbf{L})\left(\hat{I}_t \mid \theta\right) = \frac{\left(\ln\left(I_t\right) - \ln\left(\hat{I}_t\right)\right)^2}{2\left(\sigma_t^I \tilde{\sigma} / \varpi^I\right)^2} + \ln\left(\sigma_t^I \tilde{\sigma} / \varpi^I\right) + 0.5\ln\left(2\pi\right)$$

Where

(33) $$\sigma_t^I = \sqrt{\log((cv_t^I)^2 + 1)}$$

and similarly for PCPUE:

(34) $$-\ln(\mathbf{L})\left(\hat{I}2_t \mid \theta\right) = \frac{\left(\ln\left(I2_t\right) - \ln\left(\hat{I}2_t\right)\right)^2}{2\left(\sigma_t^{I2} \tilde{\sigma} / \varpi^{I2}\right)^2} + \ln\left(\sigma_t^{I2} \tilde{\sigma} / \varpi^{I2}\right) + 0.5\ln\left(2\pi\right)$$

Where

(35) $$\sigma_t^{I2} = \sqrt{\log((cv_t^{I2})^2 + 1)}$$

The distribution of the RDSI is also assumed to be normal-log and the negative log-likelihood is:

(36) $$-\ln(\mathbf{L})\left(\hat{J}_t \mid \theta\right)=\frac{\left(\ln\left(J_t\right)-\ln\left(\hat{J}_t\right)\right)^2}{2\left(\sigma_t^J \tilde{\sigma} \big/ \varpi^J\right)^2}+\ln\left(\sigma_t^J \tilde{\sigma} \big/ \varpi^J\right)+0.5\ln\left(2\pi\right)$$

Where

(37) $$\sigma_t^J = \sqrt{\log((cv_t^J)^2+1)}$$

The proportions-at-length from CSLF data are assumed to follow a multinomial distribution, with a standard deviation that depends on the effective sample size (see Section 2.2.9.3) and the weight assigned to the data:

(38) $$\sigma_{k,t}^s = \frac{\tilde{\sigma}}{\varpi^s n_t^s}$$

The negative log-likelihood is:

(39) $$-\ln(\mathrm{L})\left(\hat{p}_{k,t}^s \mid \theta\right)=\frac{p_{s,t}^s}{\sigma_{k,t}^s}\left(\ln\left(p_{k,t}^s+0.01\right)-\ln\left(\hat{p}_{k,t}^s+0.01\right)\right)$$

The likelihood for research diver sampling is analogous. Errors in the tag-recapture dataset were also assumed to be normal. For the j^{th} record, the total error is a function of the predicted standard deviation (equation (30)), observation error, and weight assigned to the data:

(40) $$\sigma_j^{tag} = \tilde{\sigma} / \varpi^{tag} \sqrt{\sigma_{obs}{}^2+\left(\sigma_j{}^d\right)^2}$$

and the negative log-likelihood is:

(41) $$-\ln(\mathbf{L})\left(\hat{d}_j \mid \theta\right)=\frac{\left(d_j-\hat{d}_j\right)^2}{2\left(\sigma_j^{tag}\right)^2}+\ln\left(\sigma_j^{tag}\right)+0.5\ln\left(2\pi\right)$$

The proportion mature-at-length was assumed to be normally distributed, with standard deviation analogous to proportions-at-length:

(42) $$\sigma_k^{mat} = \frac{\tilde{\sigma}}{\varpi^{mat}\sqrt{p_k^{mat}+0.1}}$$

The negative log-likelihood is:

(43) $$-\ln(\mathbf{L})\left(\hat{p}_k^{mat} \mid \theta\right)=\frac{\left(p_k^{mat}-\hat{p}_k^{mat}\right)^2}{2\left(\sigma_k^{mat}\right)^2}+\ln\left(\sigma_k^{mat}\right)+0.5\ln\left(2\pi\right)$$

2.2.8.2 Normalised residuals

These are calculated as the residual divided by the relevant σ term used in the likelihood. For CPUE, the normalised residual is

$$(44) \qquad \frac{\ln(I_t) - \ln(\hat{I}_t)}{\left(\sigma_t^I \tilde{\sigma} / \varpi^I\right)}$$

and similarly for PCPUE and RDSI. For the CSLF proportions-at-length, the residual is:

$$(45) \qquad \frac{p_{k,t}^s - \hat{p}_{k,t}^s}{\sigma_{k,t}^s}$$

and similarly for proportions-at-length from the RDLFs. Because the vectors of observed proportions contain many empty bins, the residuals for proportions-at-length include large numbers of small residuals, which distort the frequency distribution of residuals. When presenting normalised residuals from proportions-at-length, we arbitrarily ignore normalised residuals less than 0.05.

For tag-recapture data, the residual is:

$$(46) \qquad \frac{d_j - \hat{d}_j}{\sigma_j^{tag}}$$

and for the maturity-at-length data the residual is:

$$(47) \qquad \frac{p_k^{mat} - \hat{p}_k^{mat}}{\sigma_k^{mat}}$$

2.2.8.3 Dataset weights

Proportions at length (CSLF and RDLF) were included in the model with a multinomial likelihood. The length frequencies for individual years were assigned relative weights (effective sample size), based on a sample size that represented the best least squares fit of log(cv_i)~log(P_i), where cv_i was the bootstrap CV for the ith proportion, P_i. (See Figure A1, Appendix A, for a plot of this relationship). The weights for individual years (n_t^s for CSLF and n_t^r for RDLF) were multiplied by the weight assigned to the dataset (ϖ_s for CSLF and ϖ_r for RDLF) to obtain the model weights for the observations.

In previous assessments, the weight of the dataset was determined iteratively so that the standardised deviation of the normalised residuals was close to one. In this assessment, we used an alternative weighting scheme following Francis (2011), where the weight for the CSLF dataset was determined as

$$(48) \qquad \varpi^s = 1/\operatorname{var}_t\left[\left(\overline{O}_t^s - \overline{E}_t^s\right)/\left(v_t^s / n_t^s\right)^{0.5}\right] \quad \text{(Method TA1.8, table A1 in Francis 2011)}$$

Where

(49) $$\overline{O}_t^s = \sum_k p_{k,t}^s l_k$$

(50) $$\overline{E}_t^s = \sum_k \hat{p}_{k,t}^s l_k$$

(51) $$v_t^s = \sum_k (l_k)^2 \hat{p}_{k,t}^s - \left(\overline{E}_t^s\right)^2$$

The weight for the RDLF dataset was calculated similarly. This weighting method allows for the possibility of substantial correlations within a dataset, and generally produces relatively smaller sample sizes, thus down-weighting the composition data (Francis 2011). The actual and estimated sample sizes for the commercial catch s at length are given in Table 1.

The relative abundance indices (CPUE and RDSI) were included in the model with a lognormal likelihood. The weights for individual years were determined by the CV calculated in the standardisation and were then scaled by the weight assigned to the dataset to obtain the model weights for the observations. In previous assessments, the weight of the dataset was determined iteratively so that the standardised deviation of the normalised residuals was close to one. In this assessment, we used an alternative weighting scheme recommended by Francis (2011). With this approach, a series of lowess lines of various degrees of smoothing were fitted to the abundance indices (this is carried out outside the assessment model), and the CV of the residuals from the lowess line which is considered to have the "appropriate" smoothness is used. The CV was applied to all years in the time series and remained constant in the stock assessment model. The choice of the "appropriate" fit is based on visual examination of the lowess lines. This is equivalent to saying that we expect the stock assessment model to fit these data as well as the smoother.

2.2.8.4 Priors and bounds

Bayesian priors were established for all estimated parameters (Table 1**: Actual sample sizes, initial sample sizes determined for the multinomial likelihood, and model weighted sample sizes for the PAU 5B commercial catch sampling length frequencies from base case .**

Fishing year	Actual sample size	Initial sample size	Model 0.1 sample size
1992	18 815	3 204	176
1993	15 500	2 053	113
1994	14 706	2 464	136
1998	1 054	259	14
1999	4 656	1 259	69
2000	3 215	642	35
2001	4 145	780	43
2002	4 193	722	40
2003	4 597	1 119	62
2004	7 625	1 434	79
2005	4 656	748	41
2006	4 032	1 068	59
2007	3 537	1 173	65
2008	4 184	947	52
2009	5 016	1 565	86

2010	6 855	1 380	76
2011	5 829	785	43
2012	5 472	969	53
2013	7 331	1 050	58

Table 2). Most were incorporated simply as uniform distributions with upper and lower bounds set arbitrarily wide so as not to constrain the estimation. The prior probability density for M was a normal-log distribution with mean μ_M and standard deviation σ_M. The contribution to the objective function of estimated $M = x$ is:

$$(52) \qquad -\ln(\mathbf{L})(x \mid \mu_M, \sigma_M) = \frac{\left(\ln(M) - \ln(\mu_M)\right)^2}{2\sigma_M^{\ 2}} + \ln\left(\sigma_M \sqrt{2\pi}\right)$$

The prior probability density for the vector of estimated recruitment deviations ε, was assumed to be normal with a mean of zero and a standard deviation of 0.4. The contribution to the objective function for the whole vector is:

$$(53) \qquad -\ln\left(\mathbf{L}\right)(\varepsilon \mid \mu_\varepsilon, \sigma_\varepsilon) = \frac{\sum_{i=1}^{n_\varepsilon} \left(\varepsilon_i\right)^2}{2\sigma_\varepsilon^{\ 2}} + \ln\left(\sigma_\varepsilon\right) + 0.5\ln\left(2\pi\right).$$

Constant parameters are given in Table 3

2.2.8.5 Penalty

A penalty is applied to exploitation rates higher than the assumed maximum (equation 13; it is added to the objective function after being multiplied by an arbitrary weight (1000000) determined by experiment.

AD Model Builder™ also has internal penalties that keep estimated parameters within their specified bounds, but these should have no effect on the final outcome, because choice of a base case excludes the situations where parameters are estimated at or near a bound.

2.2.9 Fishery indicators

The assessment calculates the following quantities from their posterior distributions: the model's mid-season spawning and recruited biomass for 2013 ($B_{current}$ and $B^r_{current}$) and for the projection period (B_{proj} and B^r_{proj}).

Simulations were carried out to calculate deterministic MSY: maximum constant annual catch that can be sustained under deterministic recruitment. A single simulation run was done by starting from an unfished equilibrium state, and running under a constant exploitation rate until the catch and spawning stock biomass stabilised. For each simulation run with exploitation rate U, the equilibrium total annual catch and spawning stock biomass were calculated. The exploitation rate U that maximizes the annual catch is U_{msy}. The corresponding catch is MSY, and the corresponding SSB is B_{msy}. Together with B_o, B_{msy}, $U_{current}$, $U_{\%40B0}$ and U_{msy} the current and projected stock status is reported in relation to the following indicators:

$\%B_0$ current and projected spawning biomass as a percent of B_0

$\%B_{msy}$ current and projected spawning biomass as a percent of B_{msy}

$\Pr(> B_{current})$ Probability that projected spawning biomass is greater than $B_{current}$

$\Pr(> B_{msy})$ Probability that current and projected spawning biomass is greater than B_{msy}

$\%B_0^r$ current and projected recruited biomass as a percent of B_0^r

$\%B_{msy}^r$ current and projected recruited biomass as a percent of B_{msy}^r

$\Pr(> B_{msy}^r)$ Probability that current and projected recruit-sized biomass is greater than B_{msy}^r

$\Pr(> B_{current}^r)$ Probability that projected recruit-sized biomass is greater than $B_{current}^r$

$\Pr(B_{proj} > 40\%B_0)$ Probability that current and projected spawning biomass is greater than 40% B_0

$\Pr(B_{proj} < 20\%B_{msy})$ Probability that current and projected spawning biomass less than 20% B_0

$\Pr(B_{proj} < 10\%B_{msy})$ Probability that current and projected spawning biomass less than 10% B_0

$\Pr(U_{proj} > U_{40\%B0})$ Probability that current and projected exploitation rate greater than $U_{40\%B0}$

2.2.10 Markov chain-Monte Carlo (MCMC) procedures

AD Model Builder™ uses the Metropolis-Hastings algorithm. The step size is based on the standard errors of the parameters and their covariance relationships, estimated from the Hessian matrix.

For the MCMCs in this assessment single long chains were run, starting at the MPD estimate. The base case was 5 million simulations long and samples were saved, regularly spaced by 5000. The value of $\tilde{\sigma}$ was fixed to that used in the MPD run because it may be inappropriate to let a variance component change during the MCMC.

2.2.11 Development of base case and sensitivity model runs

Following discussions of model input data by the Shellfish Working Group (SFWG) seven initial model runs were done. These preliminary models investigated a number of weighting methods on observational datasets, alternative growth models, and various assumptions on catch histories. After reviewing the diagnostics and outputs from these models, the Shellfish WG agreed on a base case (0.1).

The base case model excluded the RDSI and RDLF data, used the methods recommended by Francis (2011) to determine the weight of the proportion-at-length and abundance data, and estimated *M* and growth within the model. In the base case, the CPUE shape parameter was fixed at 1 assuming a linear relationship between CPUE and abundance. The commercial catch history used in the base case was that estimated under "assumption 1" (between 1983–84 and 1995–96, 18%, 75%, and 7% of the catch in Statistical Area 030 was taken from PAU 5A, PAU 5B, and PAU 5D respectively, see Fu et al. (2014)).

The SFWG suggested further sensitivity runs looking at how sensitive the model is to M: Run 0.3 estimated *M* with a lognormal prior with a mean of 0.15; run 0.4 estimated *M* with a uninformative prior. Additional sensitivity runs were also carried out: Run 0.2 included the RDSI and RDLF datasets; run 0.5 used catch history estimated under "assumption 3" (between 1983–84 and 1995–96, 61%, 32%, and 7% of the catch in Statistical Area 030 was taken from PAU 5A, PAU 5B, and PAU 5D respectively, see Fu et al. (2014)); run 0.6 used the inverse-logistic growth model; Run 0.7 and 0.8 dropped the early and the recent CPUE series respectively. A summary description of base case and sensitivity model runs is given in

Table 4. The SFWG requested the MCMC runs be done with the base case and model run 0.4.

There has been a voluntary increase in the minimum harvest size (MLS) in PAU 5B (Storm Stanley per. comm.): the MLS was increased to 127 mm in 2007, 131 mm in 2009, 133 mm in 2010, and 135 mm in 2011. This step-change in MLS was modelled as an annual shift in commercial selectivity between 2007 and 2011 (see equation 11), which is equal to an annualised unit increase (D^s), multiplied by the number of units associated with each year (D_t^a). The D^s parameter was estimated within the model and D_t^a was an exogenous variable, assumed to be fixed at 1 for 2007, 3 for 2008 and 2009, 4 for 2010, and 5 for 2011. The MLS has remained at 135 mm since 2011 and therefore the commercial selectivity for 2012 and onwards was assumed to be the same as in 2011.

The sample sizes of the CSLF data were determined using the TA1.8 method (Francis 2011) and were generally less than 1% of the actual number of fish measured in the sample (**Error! Reference source not found.**). This was expected as this method accounted for the potential correlations in the proportion-at-length data and would down-weight the dataset compared to the method based on the SDNRs as used in previous assessment (see Breen & Smith 2008).

Following Francis (2011) a series of lowess lines of various degrees of smoothing were fitted to the CPUE indices. For the early CPUE (1990–2001), the residuals from the lowess line which was considered to have the "appropriate" smoothness have a CV of 0.1 (corresponding to the “f” value of 0.65 or 0.95, which represents the degree of smoothness of the lowess line, see Figure A2–left, Appendix A); for the recent CPUE (2002–2013), a CV of 0.07 was considered to be appropriate (corresponding to the “f” value of 0.80 or 0.95, see Figure A2–right, Appendix A). The CVs for the CPUE indices were fixed at those values in the assessment model.

3. RESULTS

3.1 MPD base case

Model estimates of objective function values (negative log-likelihood), parameters, and indicators for the base case are given in the first column of Table 5. The base case fitted the two observed CPUE indices very well (Figure 2) and the model appeared to have captured both the trend and inter-annual variations in the two sets of relative abundance indices. QQ plots of the residuals from the fits to the abundance indices show no apparent departure from the normality assumption (Figure 3)

Fits to commercial proportions-at-length are very reasonable (Figure 4) although fits to the left-hand side of the distribution are less adequate for the most recent three years and there is evidence of lack of fit to the plus group for the first few years. Francis (2011) suggested using the predicted annual mean length (across length classes) as a diagnostic tool for the proportion-at-length data, because of potential correlations in residuals for individual length classes. Figure 5 (left) shows a reasonable match between the predicted and observed mean length for the CSLF. The upward trend in mean length between 2006 and 2011 reflected the increase in the MLS. The midpoint of the commercial fishery selectivity was estimated to be 126 mm, and this ogive was very narrow (see Table 5). The model estimated an annual change of about 1.9 mm in commercial selectivity, with a total change of about 10 mm between 2006 and 2011 (Figure 5–right), which was in line with the increase of MLS during this period.

M was estimated to be 0.12, close to the mean of the prior distribution. Estimates of growth parameters suggested a mean annual growth of 26.2 mm at 75 mm and 7.0 mm at 120 mm (see Table 5), with a CV of 45%. Length at 50% and full maturity were estimated to be about 89 mm and 112 mm respectively (Figure 6–left). The estimated growth transition matrix appeared to have accounted for most of the variability in the growth data (Figure 6–right). Residuals from the fits to the tag-recapture data suggested that the model did not fit the small and large size classes very well (Figure 7), and this is probably because the sample size was small for these size ranges in the data.

The MPD estimates for the spawning stock biomass (mature animals) and recruited biomass (animals at or above the MLS) are shown in Figure 8. Both recruited and spawning biomass decreased substantially from 1965, but have increased fairly rapidly since 2000. The current spawning stock biomass ($B_{current}$) was estimated to be about 42% of B_0 and the current recruit-sized biomass ($B^r_{current}$) was about 35% of B^r_0 (see Table 5).

The profile likelihood on R_0 (as a proxy for B_0) indicated that the likelihood function values of the CPUE and CSLF data were sensitive to both low and high values of B_0, and the prior of *M* was also strongly influenced by the values of the initial biomass (Figure 9).

3.2 MPD sensitivity trials

Model estimates of objective function values (negative log-likelihood), parameters, and indicators for sensitivity trials are given in Table 5. A comparison of model estimates of spawning stock biomass between base case and sensitivity runs is shown in Figure 10. A comparison of model fits is shown in Figures A3–A8, Appendix A.

The inclusion of the RDSI and RDLF data appeared to have little influence on model estimates. The predicted values of RDSI and RDLF from the base model fitted the two datasets almost equally as well as model 0.2 where both datasets were included (Figures A3 and A4, Appendix A). The estimated spawning biomass were almost identical between the two models (Figure 10–first row). This suggested that the RDSI and RDLF were not in conflict with other observations. But this could also be because the RDSI and RDLF were given smaller weights.

Estimated natural mortality was 0.12 in the base case in which a lognormal prior with a mean of 0.1 was used. *M* was estimated to be 0.15 with a lognormal prior with a mean of 0.15 (Run 0.3), and 0.1 with an uninformative prior (Run 0.4). Model fits to both CPUE and CSLF have changed very little with these alternative priors (Figures A5 and A6, Appendix A), but higher biomasses were estimated, with $B_{current}$ estimated to be about 50% B_0 for both run 0.3 and 0.4 (Figure 10–second row).

Model 0.5 used a much lower catch estimates between 1985 and 1995. The model estimated higher biomass values, but a similar current depletion level to the base case (Figure 10–third row), with $B_{current}$ estimated to be about 44% B_0 (see Table 5). The fits to CPUE and CSLF data were similar to the base case.

The inverse logistic model (Run 0.6) predicted slightly smaller growth rates for the lower and higher end of the length classes (Figure A7, Appendix A), but the fits to the CSLF were similar to the base case which used the exponential growth model (Figure A8, Appendix A). This model produced higher biomass in absolute numbers, but estimates of stock size in relation to B_0 were very similar to the base case (Figure 10–fourth row).

Removing the early CPUE series (Run 0.7) had little effect, and the model estimated a similar decline in biomass between 1990 and 2001 (Figure 10–fifth row). However, removing the recent CPUE series (Run 0.8) produced a flat trend in biomass between 2002 and 2013 (Figure 10– fifth row), and estimated a much lower current stock status than the base case, with $B_{current}$ estimated to be 32% B_0.

In general, estimates of most model parameters were not significantly different among these sensitivity trials and estimates of $B_{current}$ ranged from 32% to 51% of B_0.

3.3 MCMC results

MCMC was conducted for the base case (0.1) to derive the posterior distribution of estimated parameters. The SFWG also suggested an additional MCMC run for model 0.4 in which a uniform prior was applied to M to explore the influence of the prior on the estimates of uncertainty in the stock status.

3.4 Marginal posterior distributions and the Bayesian fit

The main diagnostic used for the MCMC was the trace plots of the posterior samples for estimated parameters. For the base case the MCMC simulation started at the values of MPD estimates for model parameters and the traces show good mixing (Figure 11). The performance of the MCMC simulation was examined by running additional chains using either higher or lower starting parameter values (Figure 12). The traces of B_0 for the two additional runs stabilised after about 100 simulations and there is no evidence of non-convergence (Figure 13). The posterior distribution of key biomass indicators (B_0, $B_{current}$, and $B_{current}$ as a percent of B_0) were well formed for both MCMC 0.1 and 0.4 and the posterior medians were reasonably close to the MPD estimates (Figure 14).

The posterior distributions for estimated parameters and biomass indicators are summarised in Table 6 for the base case and in Table 6 for model 0.4. For the base case, the posterior of *M* has a median of 0.12 with a 90% credible interval between 0.11 and 0.14. The posterior median is slightly higher than that of the prior but the breadth of the posterior distribution was very similar to that of the prior (Figure 15–left). This suggested that there was information in the observations that helped inform the estimation of *M* but that the estimate was also strongly influenced by the prior. When an uninformative prior was used (MCMC 0.4), the posterior median of *M* was estimated to be 0.15, and the posterior distribution had a much wider range, with a 90% credible interval between 0.13 and 0.19 (Figure 15–right).

The estimates of recruitment deviations showed a period of relatively low recruitment through the 1990s to the early 2000s and the recruitment in recent years (after 2002) has been above the long term average (
Figure 16–left). Exploitation rates peaked around 2002, but have decreased since then
Figure 16–right). For the base case, the estimated exploitation rate in 2013 was about 0.11 (0.09–0.14).

The MCMC fits to both CPUE indices were reasonable: the posterior distribution of the predicted indices were broadly comparable to the observed indices given the error assumed for the observations (Figure 17). The posterior distributions of mean residuals (across all years) of fits to the CSLF data were not far from zero, indicating no apparent trend in the CSLF unaccounted for by the model (Figure 18–left). The QQ quantiles of the posterior residuals from the fits to the tag-recapture data showed no evidence of poor fits (Figure 18–right).

The posterior distributions of spawning stock biomass for MCMC 0.1 and 0.4 are shown in Figure 19. The base case showed that the spawning biomass increased rapidly after 2002 when the stock was at its lowest, and estimated that B_0 was about 3625 t (3392–3872t) and $B_{current}$ was about 44% (36–54%) of B_0 (Table 6). MCMC 0.4 suggested a more rapid increase in spawning biomass after 2002, and estimated that $B_{current}$ was about 55% (43–73%) of B_0 (Table 6). The posteriors of spawning stock biomass for MCMC 0.4 generally had wider bounds, indicating a higher degree of uncertainty in model estimates.

Deterministic B_{msy} was calculated using posterior samples of estimated parameters. The median of B_{msy} was estimated to be about 28% B_0 for both MCMC 0.1 and 0.4. The corresponding exploitation rate (U_{msy}) was estimated to be 37% for MCMC 0.1 and 67% for MCMC 0.4. The MLS was assumed to be fixed at 135 mm in the calculation of B_{msy}. Further investigation showed that U_{msy} was sensitive to this value and U_{msy} was estimated to be 22% for MCMC 0.1 and 31% for MCMC 0.4 when an MHS of 125 mm was used. However, both MSY and B_{msy} were less sensitive to the values of MHS. Assuming an MHS of 135 mm, $U_{\%40B_0}$ was estimated to be 19% and 30% for MCMC 0.1 and 0.4 respectively.

Estimated changes in stock size in relation to fishing pressure over-time are shown in Figure **20**. This was done by plotting the annual spawning biomass and exploitation rate as a ratio of a reference value from 1965 to 2013. Each point on the trajectory represents the estimated annual stock status: the value on the x axis is the mid-season spawning stock biomass as a ratio of either B_0 (Figure **20**–left) or B_{msy} (Figure **20**–right), the value on the y axis is the corresponding exploitation rate as a ratio $U_{\%40B_0}$ (Figure **20**–left) or U_{msy} (Figure **20**–right) for that year. The trajectory started in 1965 when the SSB is close to B_0 and the exploitation rate is close to 0. The model indicated an early phase of the fishery where the exploitation rates were below $U_{\%40B_0}$ and the SSBs were above 40% B_0 and a development phase where the exploitation rates were above $U_{\%40B_0}$ and the SSBs were below 40% B_0. The current exploitation rate is below $U_{\%40B_0}$ and the current spawning stock biomass is above 40% B_0.

3.5 Projections

Projections were made for the base case at a combination of catch levels and MHS. The two different catch levels assumed were the current catch and/or an increase of 60 t in TACC for the next three years (the projections were made to 2016). The 60 t increase in TACC was examined because this was approximately the equilibrium catch level at $U_{\%40B_0}$. The MHS assumed was either 135 mm or 125 mm. In the projection future recruitment deviations were resampled from recent model estimates (1998–2008).

Assuming the current catch level and an MLSof 135 mm the projection suggested that the spawning stock abundance will increase to about 48% (0.38–0.61) of B_0 over the next three years (Table 8, Figure 21). The projection also indicated that the probability of the spawning biomass being above the target (40% B_0) will increase from about 80% in 2013 to 93% in 2016, and that the stock status is very unlikely to be below the soft (20% B_0) or hard limit (10%) in the short term. The results changed very little when an MHS of 125 mm was assumed (Table 9).

Assuming an increase of TACC of 60 t, the projected biomass remained relatively stable over the next three years, and the probability of the spawning stock biomass being above the target (40% B_0) slightly decreased to about 74% (Table 10). The results were similar if an MHS of 125 mm was assumed (Table 11).

4. DISCUSSION

This report assesses the status of the stocks for PAU 5B and includes fishery data up to the 2012–13 fishing year. The base case model fitted the two CPUE series and the CSLF data and estimated that the current stock status was about 44% B_0 and that it was very unlikely that the stock will fall below the soft or hard limits. The projection suggested that biomass is likely to increase over the next three years at current catch levels.

The recent practice in paua stock assessment has been to exclude the research diver survey data (RDSI and RDLF) from the base case (Fu 2013). This decision was made by the Shellfish Working Group on the basis of the work by Cordue (2009) and Haist (2010) both of which suggested that the research diver survey indices were unlikely to index stock abundance at the QMA level. The research diver survey using the time-swim method has been discontinued for all paua stocks and the last survey was conducted in 2005. It has been proposed that the research diver survey be superseded by a transect-based survey which is intended to provide density estimates of paua population size (R. Naylor, NIWA, per. comm.)

The assessment used CPUE as an index of abundance. The assumption that CPUE indexes abundance is questionable. The literature on abalone suggests that CPUE is difficult to use in abalone stock assessments because of serial depletion. This can happen when fishers can deplete unfished or lightly fished beds and maintain their catch rates by moving to new areas, thus CPUE stays high while the biomass is actually decreasing. For PAU 5B, the model estimate of the stock status was strongly driven by the trend in the recent CPUE indices. It was unknown that to what extent the CPUE series tracked the stock abundance. The SFWG believed that the increasing trend in recent CPUE series may be credible, corroborating anecdotal evidence from the commercial divers in PAU 5B that the stock has been in good shape in recent years (S. Stanley, Paua Industry Council, per. comm.)

Natural mortality is a key productivity parameter. *M* can be difficult to estimate within a stock assessment model. The paua stock assessments generally estimated *M* within the model, but it has been noted that the estimate is often strongly influenced by the assumed prior. The choice of prior was based on available evidence and current belief on the plausible range of natural mortality for paua, and therefore it is reasonable to incorporate the prior to inform the estimation of *M*.

Another source of uncertainty is the catch data. The commercial catch is unknown before 1974 and is estimated with uncertainly before 1995. Although we think the effect is minor, major differences may exist between the catches we assume and what was actually taken. In addition, non-commercial catch estimates are poorly determined and could be substantially different from what was assumed, although generally non-commercial catches appear to be relatively small compared with commercial catch. The estimate of illegal catch in particular is uncertain.

The model treats the whole of the assessed area of PAU 5B as if it were a single stock with homogeneous biology, habitat and fishing pressures. The model assumes homogeneity in recruitment and natural mortality, and that growth has the same mean and variance. However it is known that paua in some areas have stunted growth, and others are fast-growing.

Heterogeneity in growth can be a problem for this kind of model (Punt 2003). Variation in growth is addressed to some extent by having a stochastic growth transition matrix based on increments observed in several different places; similarly the length frequency data are integrated across samples from many places. One potential effect is that model results could be more optimistic. For instance, if some local stocks are fished very hard and others not fished, recruitment failure can result because of the depletion of spawners. Spawners must breed close to each other and the dispersal of larvae is unknown and may be limited. Recruitment failure is a common observation in overseas abalone fisheries, so local processes may decrease recruitment, an effect that the current model cannot account for.

Another source of uncertainty is that fishing may cause spatial contraction of populations (Shepherd & Partington 1995), or that some populations become relatively unproductive after initial fishing (Gorfine & Dixon 2000). If this happens, the model will overestimate productivity in the population as a whole.. However, there is no clear evidence in the fishery data to suggest this has happened or is happening in PAU 5B.

5. ACKNOWLEDGMENTS

This work was supported by a contract from the Ministry for Primary Industries (PAU201304 Objective 1). Thank you to Paul Breen for developing the stock assessment model that was used in this assessment and for the use of major proportions of the 2006 report for this update. Thank you to the Shellfish Working Group for all the advice provided throughout the assessment process. Thank you to Reyn Naylor for reviewing the draft report.

6. REFERENCES

Andrew, N.L.; Breen, P.A.; Naylor, J.R.; Kendrick, T.H.; Gerring, P. (2000). Stock assessment of paua (*Haliotis iris*) in PAU 7 in 1998–99. *New Zealand Fisheries Assessment Report 2000/49*. 40 p.

Breen, P.A.; Andrew, N.L.; Kendrick, T.H. (2000a). Stock assessment of paua (*Haliotis iris*) in PAU 5B and PAU 5D using a new length-based model. *New Zealand Fisheries Assessment Report 2000/33*. 37 p.

Breen, P.A.; Andrew, N.L.; Kendrick, T.H. (2000b). The 2000 stock assessment of paua (*Haliotis iris*) in PAU 5B using an improved Bayesian length-based model. *New Zealand Fisheries Assessment Report 2000/48*. 36 p.

Breen, P.A.; Andrew, N.L.; Kim, S.W. (2001). The 2001 stock assessment of paua (*Haliotis iris*) in PAU 7. *New Zealand Fisheries Assessment Report 2001/55*. 53 p.

Breen, P.A.; Kim, S.W. (2003). The 2003 stock assessment of paua (*Haliotis iris*) in PAU 7. *New Zealand Fisheries Assessment Report 2003/35.* 112 p.

Breen, P.A.; Kim, S.W. (2004a). The 2004 stock assessment of paua (*Haliotis iris*) in PAU 4. *New Zealand Fisheries Assessment Report 2004/55.* 79 p.

Breen, P.A.; Kim, S.W. (2004b). The 2004 stock assessment of paua (*Haliotis iris*) in PAU 5A. *New Zealand Fisheries Assessment Report 2004/40*. 86 p.

Breen, P.A.; Kim, S.W. (2005). The 2005 stock assessment of paua (*Haliotis iris*) in PAU 7. *New Zealand Fisheries Assessment Report 2005/47.* 114 p.

Breen, P.A.; Kim, S.W. (2007). The 2006 stock assessment of paua (*Haliotis iris*) stocks PAU 5A (Fiordland) and PAU 5D (Otago). *New Zealand Fisheries Assessment Report 2007/09*. 164 p.

Breen, P.A.; Kim, S.W.; Andrew, N.L. (2003). A length-based Bayesian stock assessment model for abalone. *Marine and Freshwater Research 54(5):* 619–634.

Breen, P.A.; Smith, A.N.H. (2008). The 2007 assessment for paua *(Haliotis iris)* stock PAU 5B (Stewart Island). *New Zealand Fisheries Assessment Report 2008/05.*

Bull, B.; Francis, R.I.C.C.; Dunn, A.; McKenzie, A.; Gilbert, D.J.; Smith, M.H.; Bian, R. (2012). CASAL (C++ algorithmic stock assessment laboratory): CASAL User Manual v2.30-2012/03/21. NIWA Technical Report 135.

Cordue, P.L. (2009). Analysis of PAU5A dive survey data and PCELR catch and effort data. Final report for SeaFIC and PauaMAC5. (Unpublished report held by SeaFIC.)

Francis, R.I.C.C. (2011). Data weighting in statistical fisheries stock assessment models. *Canadian Journal of Fisheries and Aquatic Sciences* 68: 15.

Fu, D. (2012). The 2011 stock assessment of paua (*Haliotis iris*) for PAU 7. *New Zealand Fisheries Assessment Report 2012/27*. 56 p.

Fu, D. (2013). The 2012 stock assessment of paua (*Haliotis iris*) for PAU 5D. *New Zealand Fisheries Assessment Report 2013/57*. 56 p.

Fu, D.; McKenzie, A. (2010a). The 2010 stock assessment of paua (*Haliotis iris*) for Chalky and South Coast in PAU 5A. *New Zealand Fisheries Assessment Report 2010/36.* 63 p.

Fu, D.; McKenzie, A. (2010b). The 2010 stock assessment of paua (*Haliotis iris*) for Milford, George, Central, and Dusky in PAU 5A. *New Zealand Fisheries Assessment Report 2010/46*. 55 p.

Fu, D.; McKenzie, A; Naylor, R. (2014). Summary of input data for the 2013 PAU 5B stock assessment. *New Zealand Fisheries Assessment Report 2014/43*. 61 p

Gorfine, H.K.; Dixon, C.D. (2000). A behavioural rather than resource-focused approach may be needed to ensure sustainability of quota managed abalone fisheries. *Journal of Shellfish Research* 19: 515–516.

Haist, V. (2010). Paua research diver survey: review of data collected and simulation study of survey method. *New Zealand Fisheries Assessment Report 2010/38*. 54 p.

Kim, S.W.; Bentley, N.; Starr, P.J.; Breen, P.A. (2004). Assessment of red rock lobsters (*Jasus edwardsii*) in CRA 4 and CRA 5 in 2003. *New Zealand Fisheries Assessment Report 2004/8.* 165 p.

McKenzie, A.; Smith, A.N.H. (2009). The 2008 stock assessment of paua (*Haliotis iris*) in PAU 7. *New Zealand Fisheries Assessment Report 2009/34.* 84 p.

McShane, P.E.; Mercer, S.F.; Naylor, J.R. (1994). Spatial variation and commercial fishing of the New Zealand paua (*Haliotis iris* and *H. australis*). *New Zealand Journal of Marine and Freshwater Research* 28: 345–355.

McShane, P.E.; Mercer, S.; Naylor, J.R.; Notman, P.R. (1996): Paua (*Haliotis iris*) fishery assessment in PAU 5, 6, and 7. New Zealand Fisheries Assessment Research Document 96/11. 35 p. (Unpublished report held in NIWA library, Wellington.)

Punt, A.E. (2003). The performance of a size-structured stock assessment method in the face of spatial heterogeneity in growth. *Fisheries Research 65:* 391–409.

Schiel, D.R. (1989). Paua fishery assessment 1989. New Zealand Fisheries Assessment Research Document 89/9: 20 p. (Unpublished report held in NIWA library, Wellington, New Zealand.)

Schiel, D.R. (1992). The paua (abalone) fishery of New Zealand. *In:* Abalone of the world: Biology, fisheries and culture. Shepherd, S.A.; Tegner, M.J.; Guzman del Proo, S. (eds.) pp. 427–437. Blackwell Scientific, Oxford.

Schiel, D.R.; Breen, P.A. (1991). Population structure, ageing and fishing mortality of the New Zealand abalone *Haliotis iris*. *Fishery Bulletin 89*: 681–691.

Shepherd, S.A.; Breen, P.A. (1992). Mortality in abalone: its estimation, variability and causes. *In*: ‘Abalone of the World: Biology, Fisheries and Culture’. (Eds S.A. Shepherd, M.J. Tegner, and S. Guzman del Proo.) pp. 276–304. (Blackwell Scientific: Oxford.)

Shepherd, S.A.; Partington, D. (1995). Studies on Southern Australian abalone (genus Haliotis). XVI. Recruitment, habitat and stock relations. *Marine and Freshwater Research 46*: 669–680.

Shepherd, S.A.; Rodda, K.R.; Vargas, K.M. (2001). A chronicle of collapse in two abalone stocks with proposals for precautionary management. *Journal of Shellfish Research 20:* 843–856.

Table 1: Actual sample sizes, initial sample sizes determined for the multinomial likelihood, and model weighted sample sizes for the PAU 5B commercial catch sampling length frequencies from base case .

Fishing year	Actual sample size	Initial sample size	Model 0.1 sample size
1992	18 815	3 204	176
1993	15 500	2 053	113
1994	14 706	2 464	136
1998	1 054	259	14
1999	4 656	1 259	69
2000	3 215	642	35
2001	4 145	780	43
2002	4 193	722	40
2003	4 597	1 119	62
2004	7 625	1 434	79
2005	4 656	748	41
2006	4 032	1 068	59
2007	3 537	1 173	65
2008	4 184	947	52
2009	5 016	1 565	86
2010	6 855	1 380	76
2011	5 829	785	43
2012	5 472	969	53
2013	7 331	1 050	58

Table 2: Base case model specifications: for estimated parameters, the phase of estimation, type of prior, (U, uniform; N, normal; LN, lognormal), mean and CV of the prior, lower bound and upper bound.

Parameter	Phase	Prior	μ	CV	Bounds	
					Lower	Upper
ln($R0$)	1	U	–	–	5	50
M	3	LN	0.1	0.35	0.01	0.5
g_1	2	U	–	–	1	50
$g2$	2	U	–	–	0.01	50
φ	2	U	–	–	0.001	1
$Ln(q^I)$	1	U	–	–	-30	0
$Ln(q^J)$	1	U	–	–	-30	0
$Ln(q^k)$	1	U	–	–	-30	0
L_{50}	1	U	–	–	70	145
L_{95-50}	1	U	–	–	1	50
T_{50}	2	U	–	–	70	125
T_{95-50}	2	U	–	–	0.001	50
D_{50}	2	U	–	–	70	145
D_{95-50}	2	U	–	–	0.01	50
ε	1	N	0	0.4	-2.3	2.3
D^s	1	U	–	–	0.01	10

Table 3: Values for fixed quantities for base case model.

Variable	Value
L_1	75
L_2	120
a	2.99E-08
b	3.303
U^{max}	0/80
σ_{min}	1
σ_{obs}	0.25
$\tilde{\sigma}$	0.2
H	0.75

Table 4: Summary descriptions for MPD base case and sensitivity runs.

Model	Description
0.1 (base case)	Excluded RDSI and RDLF, Francis (2011) weighting method on CSLF and CPUE, exponential growth model
0.2	0.1, included RDSI and RDLF
0.3	0.1, estimated M using a lognormal prior with a mean of 0.15
0.4	0.1, estimated M using an uninformative prior
0.5	0.1, using the lower values of the estimated commercial catch history
0.6	0.1, using the inverse-logistic growth model
0.7	0.1, dropped the early CPUE series
0.8	0.1, dropped the recent CPUE series

Table 5: MPD estimates for base case and sensitivity trials. Red indicates parameter fixed and likelihood contributions not used when datasets were removed. SDNRs for CSLF were calculated from mean length for runs using TA.18 weighting method.

								Model runs
	0.1	0.2	0.3	0.4	0.5	0.6	0.7	0.8
Likelihoods								
CPUE	-13.3	-13.7	-13.3	-13.3	-13.5	-12.8	-11.5	-13.4
PCPUE	-14.6	-14.5	-14.6	-14.6	-14.6	-15.2	-14.6	64.5
RDSI	2.2	1.5	3.4	3.1	3.1	4.1	3.4	1.8
CSLF	34.1	32.2	31.4	31.6	34.2	20.9	34.1	34.2
RDLF	8.9	7.1	9.1	9.0	8.8	10.3	9.9	9.2
Tags	940.5	940.5	940.7	940.6	940.5	936.0	940.4	940.6
Maturity	-28.8	-28.8	-28.8	-28.8	-28.8	-28.8	-28.8	-28.8
Prior on M	0.4	0.2	-1.4	0.0	0.5	-1.2	0.5	-0.2
Prior on ε	4.3	4.6	5.3	5.1	3.9	3.5	3.7	5.7
U penalty	0.0	0.0	0.0	0.0	0.0	0.0	0.0	0.0
ε penalty	0.0	0.0	0.0	0.0	0.0	0.0	0.0	0.0
Total	922.5	929.0	919.3	920.7	922.3	902.5	935.3	938.2
Parameters								
ln($R0$)	14.0	14.0	14.2	14.1	13.9	13.9	14.0	13.9
M	0.121	0.119	0.147	0.143	0.121	0.107	0.122	0.117
T_{50}	89.1	89.1	89.1	89.1	89.1	89.1	89.1	89.1
T_{95-50}	23.8	23.8	23.8	23.8	23.8	23.8	23.8	23.8
D_{50}	125.9	125.8	125.9	125.9	125.9	125.5	125.8	125.6
D_{95-50}	3.8	3.7	3.8	3.8	3.8	3.3	3.7	3.6
D^s	1.9	1.9	2.0	2.0	1.9	1.9	1.9	2.1
L_{50}	111.8	111.8	111.8	111.8	111.8	111.8	111.8	111.8
L_{95-50}	33.4	33.4	33.4	33.4	33.4	33.4	33.4	33.4
ln(q^I)	-13.4	-13.4	-13.5	-13.5	-13.3	-13.6	-13.4	-13.4
ln(q^{I2})	-13.4	-13.4	-13.5	-13.5	-13.3	-13.6	-13.5	-13.4
ln(q^J)	-14.7	-14.7	-14.7	-14.7	-14.7	-14.7	-14.7	-14.7
g_α	26.2	25.8	25.7	25.8	26.0	–	26.4	26.8
g_β	7.0	7.0	7.1	7.1	7.1	–	6.9	6.8
φ	0.45	0.45	0.45	0.45	0.45	0.45	0.45	0.45
g_{max}	–	–	–	–	–	35.1	–	–
$g_{50\%}$	–	–	–	–	–	89.0	–	–
$g_{50-95\%}$	–	–	–	–	–	65.6	–	–

Table 5 continued

Indicators								
B_0	3572	3583	3301	3335	3360	3925	3613	3449
$B_{current}$	1488	1446	1693	1660	1380	1703	1593	1120
$B_{current}/B_0$	0.42	0.40	0.51	0.50	0.41	0.43	0.44	0.32
B^r_0	3149	3165	2813	2857	2963	3496	3180	3049
$B^r_{current}$	1118	1082	1247	1226	1033	1323	1208	789
$B^r_{current}/B^r_0$	0.35	0.34	0.44	0.43	0.35	0.38	0.38	0.26
$U_{current}$	0.12	0.12	0.11	0.11	0.13	0.10	0.11	0.18
Weights								
CPUE	0.20	0.20	0.20	0.20	0.20	0.20	0.20	0.20
PCPUE	0.20	0.20	0.20	0.20	0.20	0.20	0.20	0.20
RDSI	–	0.20	–	–	–	–	–	–
CSLF	0.01	0.01	0.01	0.01	0.01	0.01	0.01	0.01
RDLF	–	0.01	–	–	–	–	–	–
Tags	0.20	0.20	0.20	0.20	0.20	0.20	0.20	0.20
Maturity	3.03	3.03	3.03	3.03	3.03	3.03	3.03	3.03
SDNRs								
CPUE	0.74	0.70	0.74	0.74	0.72	0.80	0.90	0.73
PCPUE	1.02	1.03	1.03	1.02	1.02	0.97	1.02	2.97
RDSI	–	1.34	–	–	–	–	–	–
CSLF	1.00	0.99	1.03	0.98	0.98	0.98	0.33	0.34
RDLF	–	0.98	–	–	–	–	–	–
Tags	1.05	1.05	1.05	1.05	1.05	1.05	1.05	1.06
Maturity	1.00	1.00	1.00	1.00	1.00	1.00	1.00	1.00

Table 6: Summary of the marginal posterior distributions from the MCMC chain from the base case (0.1). The columns show the minimum values observed in the 1000 samples, the maxima, the 5th and 95th percentiles, and the medians. Biomass is in tonnes.

	Min	5%	Median	95%	Max
Parameters					
f	930.1	936.3	943.0	951.4	966.2
ln(*R0*)	13.8	13.9	14.0	*14.1*	14.3
M	0.095	0.110	0.122	*0.136*	0.155
D_{50}	124.2	125.2	125.9	*126.6*	127.6
$D_{95\text{-}50}$	1.0	2.7	3.9	*5.3*	7.5
D^s	1.5	1.7	1.9	2.2	2.4
L_{50}	85.1	87.3	89.0	90.5	92.4
$L_{95\text{-}50}$	16.3	20.5	24.2	*28.4*	33.4
$\ln(q^I)$	-13.9	-13.7	-13.5	*-13.3*	-13.0
$\ln(q^{II})$	-14.1	-13.7	-13.5	*-13.2*	-12.9
g_α	21.8	24.4	26.6	*29.1*	32.3
g_β	6.1	6.5	6.8	7.3	8.0
φ	0.37	0.43	0.46	0.51	0.56
Indicators					
B_0	3061	3392	3625	3872	4254
B_{msy}	876	960	1021	1086	1195
$B_{current}$	965	1293	1592	1975	2636
$B_{current}/B_0$	0.27	0.36	0.44	0.53	0.67
$B_{current}/B_{msy}$	0.94	1.28	1.56	1.90	2.40
B_{msy}/B_0	0.27	0.28	0.28	0.29	0.29
B_0^r	2645	2952	3194	3440	3812
B_{msy}^r	487	587	664	737	830
$B_{current}^r$	692	953	1210	1534	2127
$B_{current}^r/B_0^r$	0.22	0.30	0.38	0.47	0.62
$B_{current}^r/B_{msy}^r$	0.93	1.40	1.82	2.39	3.29
B_{msy}^r/B_0^r	0.18	0.19	0.21	0.22	0.23
MSY	146	156	166	182	208
U_{msy}	0.23	0.29	0.37	0.50	0.79
$U_{40\%B_0}$	0.14	0.16	0.19	0.24	0.34
$U_{current}$	0.06	0.09	0.11	0.14	0.18

Table 7: Summary of the marginal posterior distributions from the MCMC chain from model 0.4. The columns show the minimum values observed in the 1000 samples, the maxima, the 5th and 95th percentiles, and the medians. Biomass is in tonnes.

	Min	5%	Median	95%	Max
Parameters					
f	924.2	930.8	937.4	946.1	959.9
ln(*R0*)	13.8	14.0	14.2	*14.6*	15.2
M	0.105	0.126	0.152	*0.194*	0.270
D_{50}	124.5	125.2	125.8	*126.5*	127.4
D_{95-50}	1.3	2.6	3.8	*5.2*	7.2
D^s	1.5	1.8	2.0	2.2	2.5
L_{50}	85.3	87.2	89.0	90.5	92.2
L_{95-50}	16.1	20.6	24.1	*28.2*	32.9
$\ln(q^I)$	-14.1	-13.8	-13.6	*-13.3*	-13.1
$\ln(q^{II})$	-14.2	-13.9	-13.6	*-13.3*	-13.0
g_α	21.7	23.9	25.9	*28.4*	32.2
g_β	6.2	6.6	7.0	7.4	7.9
φ					
Indicators					
B_0	2664	3063	3366	3691	4104
B_{msy}	792.6	887	967	1119	1592
$B_{current}$	1049	1441	1855	2486	3616
$B_{current}/B_0$	0.3	0.43	0.55	0.73	0.93
$B_{current}/B_{msy}$	1.15	1.52	1.94	2.31	2.69
B_{msy}/B_0	0.27	0.28	0.28	0.34	0.47
B_0^r	2083	2490	2838	3185	3550
B_{msy}^r	375	448	534	648	762
$B_{current}^r$	732	1045	1375	1851	2747
$B_{current}^r/B_0^r$	0.3	0.37	0.49	0.67	0.91
$B_{current}^r/B_{msy}^r$	1.2	1.79	2.64	3.48	4.30
B_{msy}^r/B_0^r	0.2	0.17	0.19	0.21	0.29
MSY	150	167	190	234	308
U_{msy}	0.27	0.39	0.67	0.98	0.98
$U_{\%40B_0}$	0.15	0.20	0.30	0.56	0.98
$U_{current}$	0.05	0.07	0.10	0.13	0.18

Table 8: Summary of key indicators from the projection for the base case (0.1) MCMC with future commercial catch set to current TACC and future minimum harvest size set to 135 mm: projected biomass as a percentage of the virgin and current stock status, for spawning stock and recruit-sized biomass.

	2013	2014	2015	2016
$B_{proj}\%B_0$	0.44 (0.35–0.55)	0.45 (0.36–0.57)	0.47 (0.37–0.58)	0.48 (0.38–0.61)
$B_{proj}\%B_{msy}$	1.56 (1.24–1.97)	1.61 (1.27–2.03)	1.65 (1.30–2.10)	1.69 (1.32 –2.18)
$\Pr(>B_{msy})$	1.00	1.00	1.00	1.00
$\Pr(>B_{current})$	0.00	0.90	0.91	0.92
$\Pr(>40\%B_0)$	0.80	0.86	0.90	0.93
$\Pr(<20\%B_0)$	0.00	0.00	0.00	0.00
$\Pr(<10\%B_0)$	0.00	0.00	0.00	0.00
$\%B_0^r$	0.38 (0.29–0.49)	0.39 (0.31–0.51)	0.41 (0.32–0.52)	0.42 (0.33–0.53)
$\%B_{msy}^r$	1.82 (1.34–2.53)	1.89 (1.40–2.61)	1.96(1.46–2.68)	2.02 (1.51–2.74)
$\Pr(>B_{msy}^r)$	1.00	1.00	1.00	1.00
$\Pr(>B_{current}^r)$	–	1.00	1.00	1.00
$\Pr(U_{proj}>U_{40\%B0})$	0.14	0.08	0.04	0.02

Table 9: Summary of key indicators from the projection for the base case (0.1) MCMC with future commercial catch set to current TACC and future minimum harvest size set to 125 mm: projected biomass as a percentage of the virgin and current stock status, for spawning stock and recruit-sized biomass.

	2013	2014	2015	2016
$B_{proj}\%B_0$	0.44 (0.35–0.55)	0.45 (0.36–0.57)	0.46 (0.37–0.58)	0.47 (0.37–0.61)
$B_{proj}\%B_{msy}$	1.59 (1.26–2.03)	1.64 (1.30–2.09)	1.69 (1.32–2.15)	1.72 (1.34–2.23)
$\Pr(>B_{msy})$	1.00	1.00	1.00	1.00
$\Pr(>B_{current})$	0.00	0.90	0.91	0.91
$\Pr(>40\%B_0)$	0.79	0.85	0.89	0.92
$\Pr(<20\%B_0)$	0.00	0.00	0.00	0.00
$\Pr(<10\%B_0)$	0.00	0.00	0.00	0.00
$\%B_0^r$	0.38 (0.29–0.49)	0.39 (0.31–0.51)	0.41 (0.32–0.52)	0.419 (0.33–0.53)
$\%B_{msy}^r$	1.87 (1.36–2.62)	1.94 (1.43–2.70)	2.01 (1.48–2.77)	2.07 (1.54–2.84)
$\Pr(>B_{msy}^r)$	1.00	1.00	1.00	1.00
$\Pr(>B_{current}^r)$	0.00	1.00	1.00	1.00
$\Pr(U_{proj}>U_{40\%B0})$	0.14	0.00	0.00	0.00

Table 10: Summary of key indicators from the projection for the base case (0.1) MCMC with future commercial catch set to current TACC plus 60 t and future minimum harvest size set to 135 mm: projected biomass as a percentage of the virgin and current stock status, for spawning stock and recruit-sized biomass.

	2013	2014	2015	2016
$B_{proj}\%B_0$	0.44 (0.35–0.55)	0.44 (0.35–0.560)	0.44 (0.35–0.56)	0.44 (0.34–0.57)
$B_{proj}\%B_{msy}$	1.56 (1.24–1.97)	1.57 (1.24–2.00)	1.56 (1.21–2.01)	1.55 (1.18–2.04)
$\Pr(>B_{msy})$	1.00	1.00	1.00	1.00
$\Pr(>B_{current})$	0.00	0.62	0.49	0.44
$\Pr(>40\%B_0)$	0.79	0.81	0.77	0.74
$\Pr(<20\%B_0)$	0.00	0.00	0.00	0.00
$\Pr(<10\%B_0)$	0.00	0.00	0.00	0.00
$\%B_0^r$	0.38 (0.29–0.49)	0.38 (0.30–0.50)	0.38 (0.29–0.49)	0.38 (0.28–0.49)
$\%B_{msy}^r$	1.82 (1.34–2.53)	1.85 (1.36–2.56)	1.83 (1.34–2.54)	1.81 (1.30–2.52)
$\Pr(>B_{msy}^r)$	1.00	1.00	1.00	1.00
$\Pr(>B_{current}^r)$	0.00	1.00	0.59	0.36
$\Pr(U_{proj}>U_{40\%B0})$	0.14	0.87	0.88	0.8888

Table 11: Summary of key indicators from the projection for the base case (0.1) MCMC with future commercial catch set to current TACC plus 60 t and future minimum harvest size set to 125 mm: projected biomass as a percentage of the virgin and current stock status, for spawning stock and recruit-sized biomass.

	2013	2014	2015	2016
$B_{proj}\%B_0$	0.44 (0.35–0.55)	0.44 (0.35–0.56)	0.44 (0.35–0.56)	0.43 (0.33–0.57)
$B_{proj}\%B_{msy}$	1.59 (1.26–2.03)	1.61 (1.27–2.06)	1.60 (1.23–2.07)	1.58 (1.19–2.09)
$\Pr(>B_{msy})$	1.00	1.00	1.00	1.00
$\Pr(>B_{current})$	0.00	0.62	0.48	0.42
$\Pr(>40\%B_0)$	0.79	0.81	0.77	0.73
$\Pr(<20\%B_0)$	0.00	0.00	0.00	0.00
$\Pr(<10\%B_0)$	0.00	0.00	0.00	0.00
$\%B_0^r$	0.38 (0.29–0.49)	0.38 (0.30–0.50)	0.38 (0.29–0.49)	0.37 (0.28–0.49)
$\%B_{msy}^r$	1.87 (1.36–2.62)	1.90 (1.38–2.65)	1.88 (1.36–2.63)	1.85 (1.33–2.61)
$\Pr(>B_{msy}^r)$	1.00	1.00	1.00	1.00
$\Pr(>B_{current}^r)$	0.00	1.00	0.57	0.32
$\Pr(U_{proj}>U_{40\%B0})$	0.14	0.35	0.37	0.40

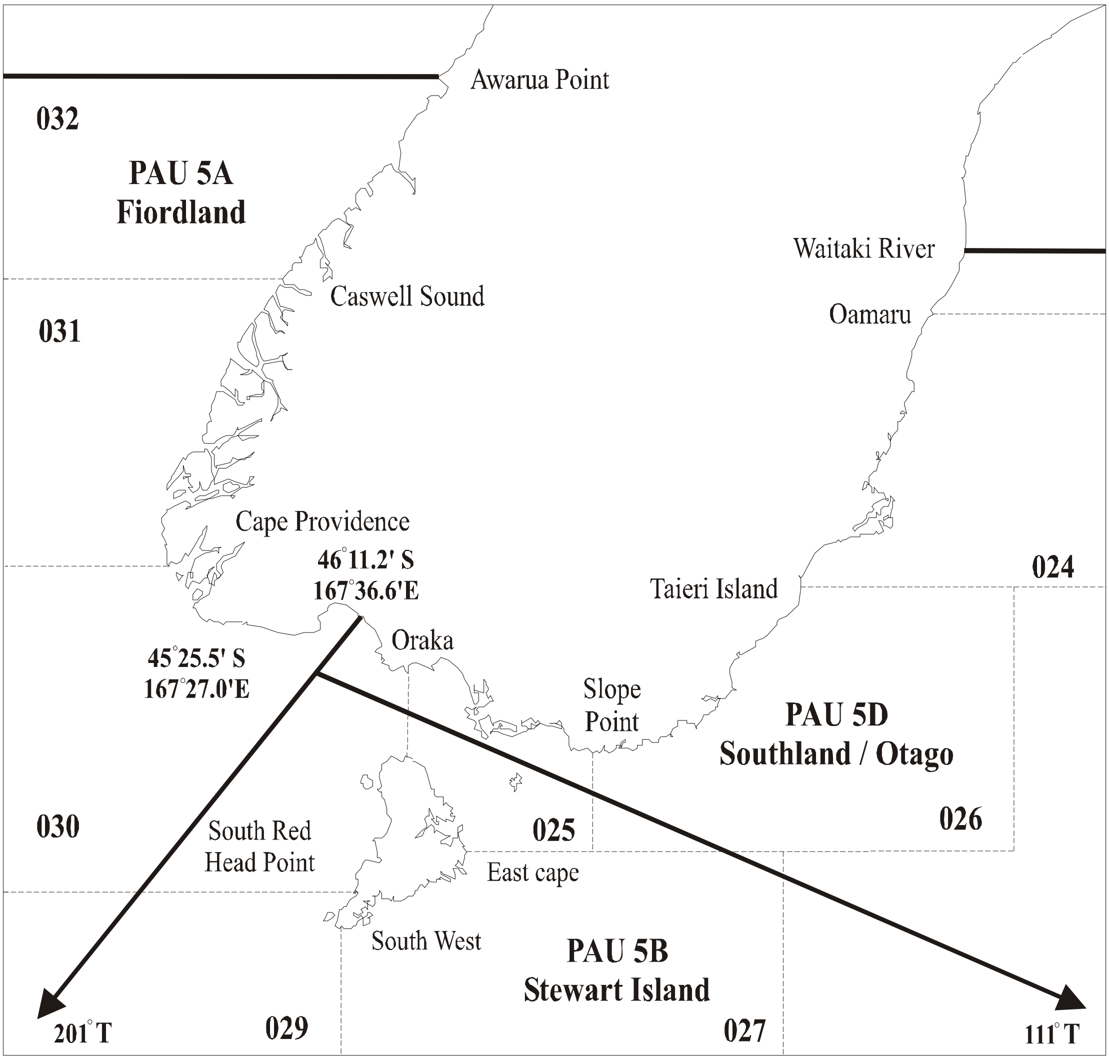

Figure 1: Map of PAU 5 showing the boundaries of the general statistical areas.

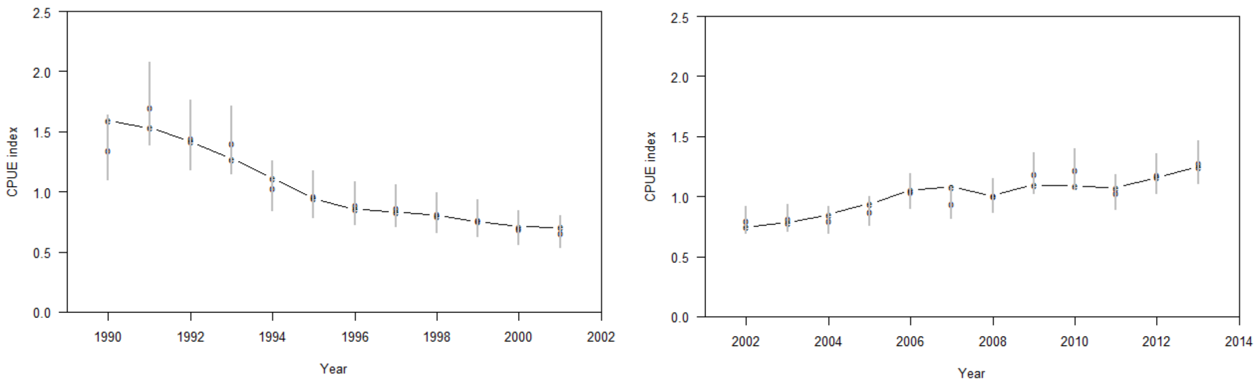

Figure 2: MPD fits to the CPUE indices (left) and PCPUE indices (right), for the base case model (0.1).

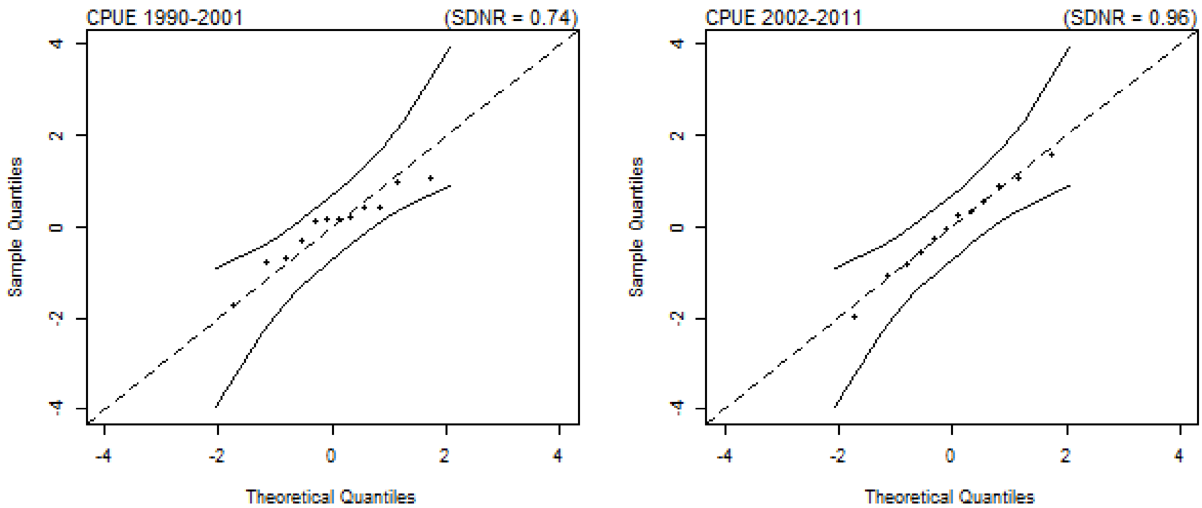

Figure 3: Normal Q-Q plots for residuals from fits to the two CPUE datasets for the MPD base case model (0.1).

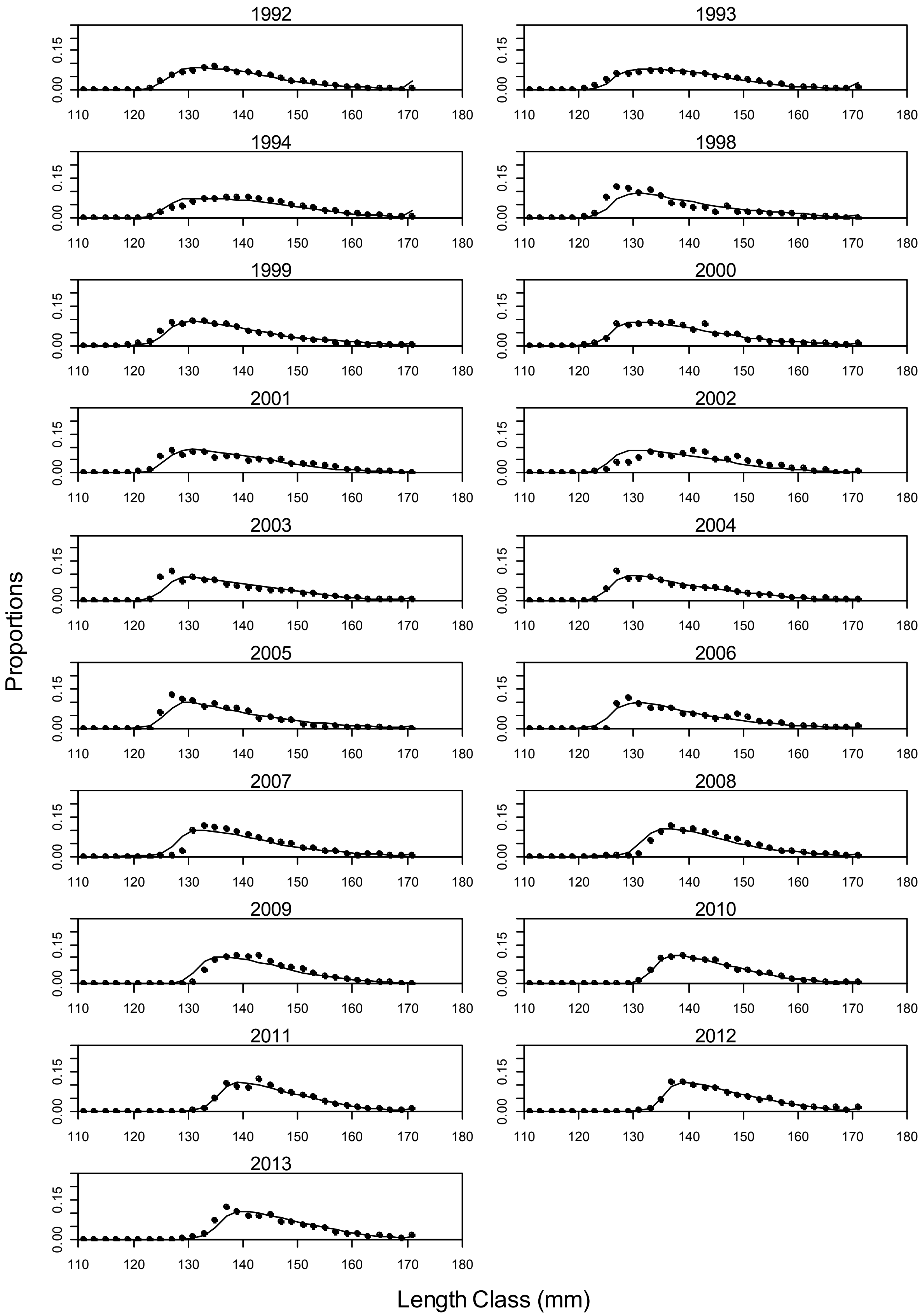

Figure 4: MPD fits to the CSLF data for the base case model (0.1).

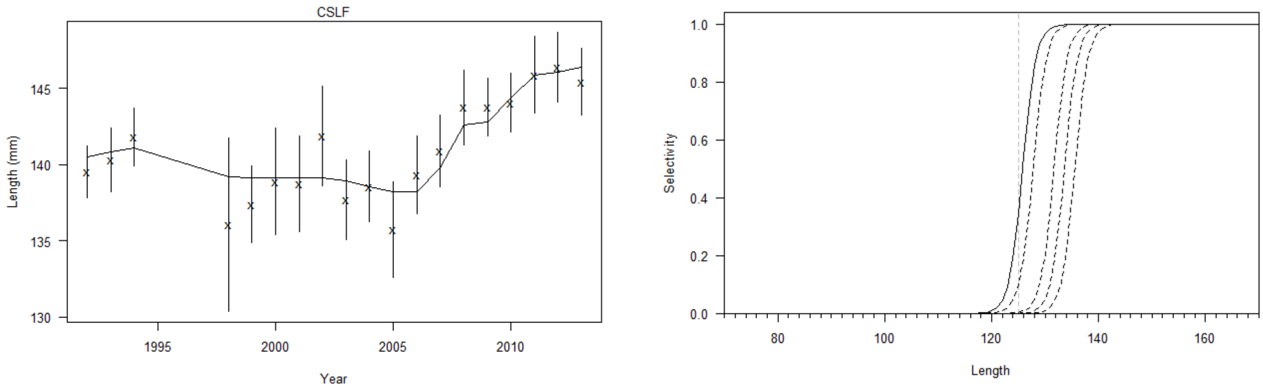

Figure 5: Estimated commercial catch selectivity (left) and observed and predicted mean length by year for the CSLF datasets for MPD base case model (0.1). The selectivity was shifted incrementally in 2007, 2008, 2010, and 2011. The vertical lines are confidence intervals for the mean length.

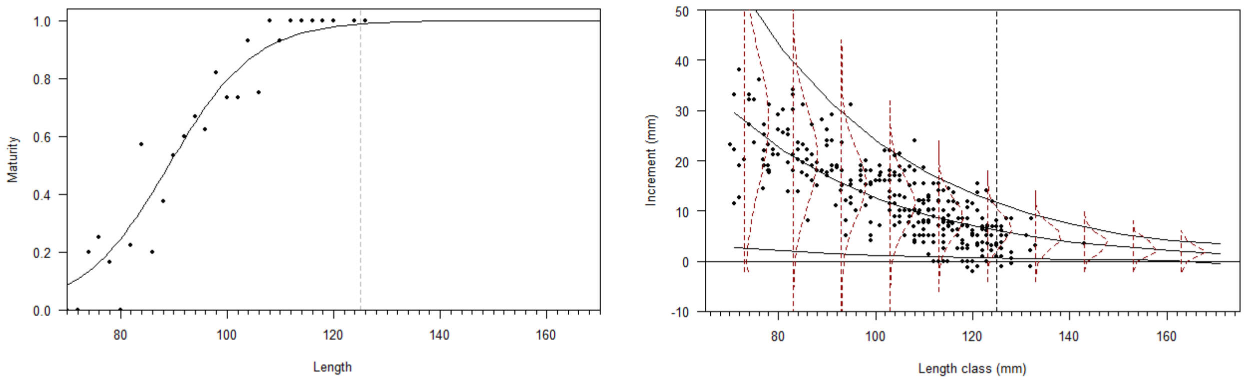

Figure 6: MPD fits to the maturity data (left: dots are observed proportion mature at length with confidence interval; the line is predicted proportion of maturity at length) and the tag-recapture data (right: The dots are observed mean annual increments; the black lines are the fitted growth curve with 95% confidence intervals; dashed lines are from the estimated growth transition matrix at selected sizes) for base case model (0.1).

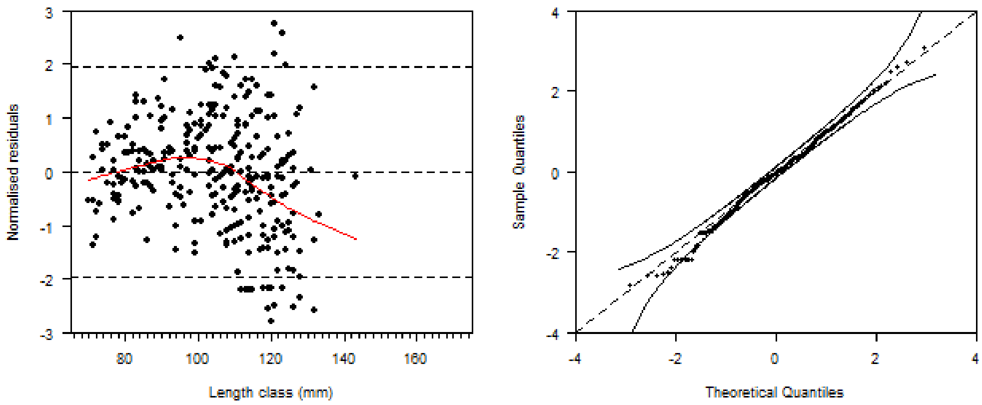

Figure 7: Normalised residuals by length class (left) and Normal Q-Q plot from the fits to the tag-recapture data for the base case model (0.1).

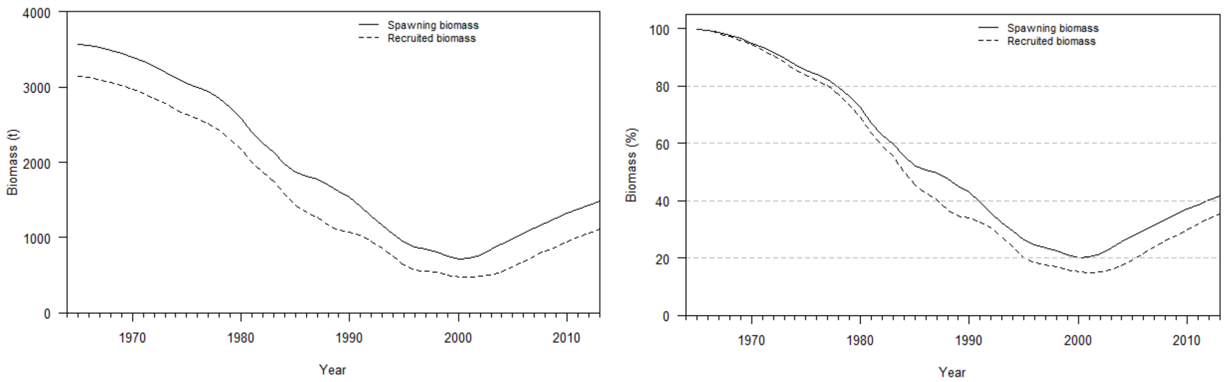

Figure 8: Estimated spawning and recruit-sized biomass (left) and spawning and recruit-sized biomass as a percentage of the virgin level (right) for MPD base case model (0.1).

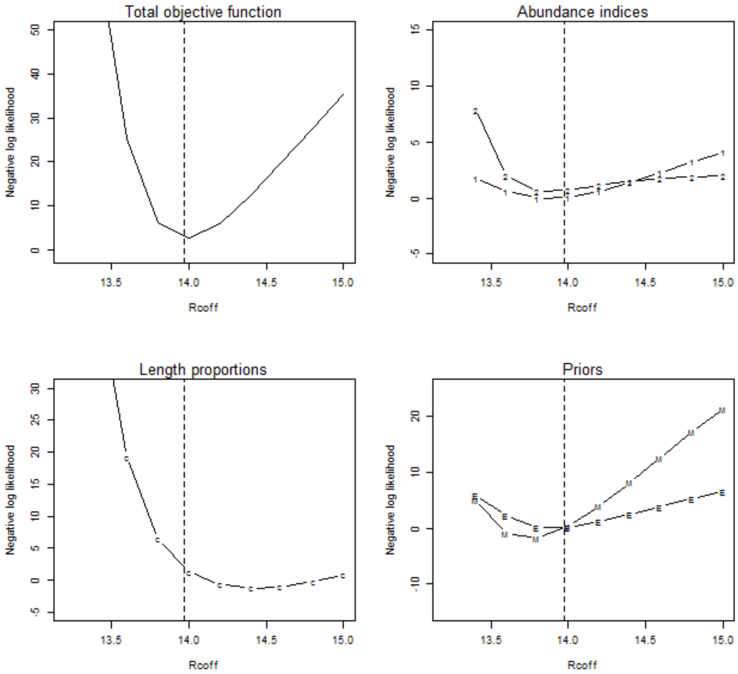

Figure 9: Profile likelihood for parameter $\ln(R0)$ for the base case model (0.1). The profile likelihood is shown for the total objective function value (top left), component likelihood (top right for the CPUE ("1" for CELR and "2" for PCELR), and bottom left for the CSLF), and for the prior (bottom right, E represents prior on the recruitment deviation and *M* represents prior on the natural mortality). Dashed line represents the minimum value.

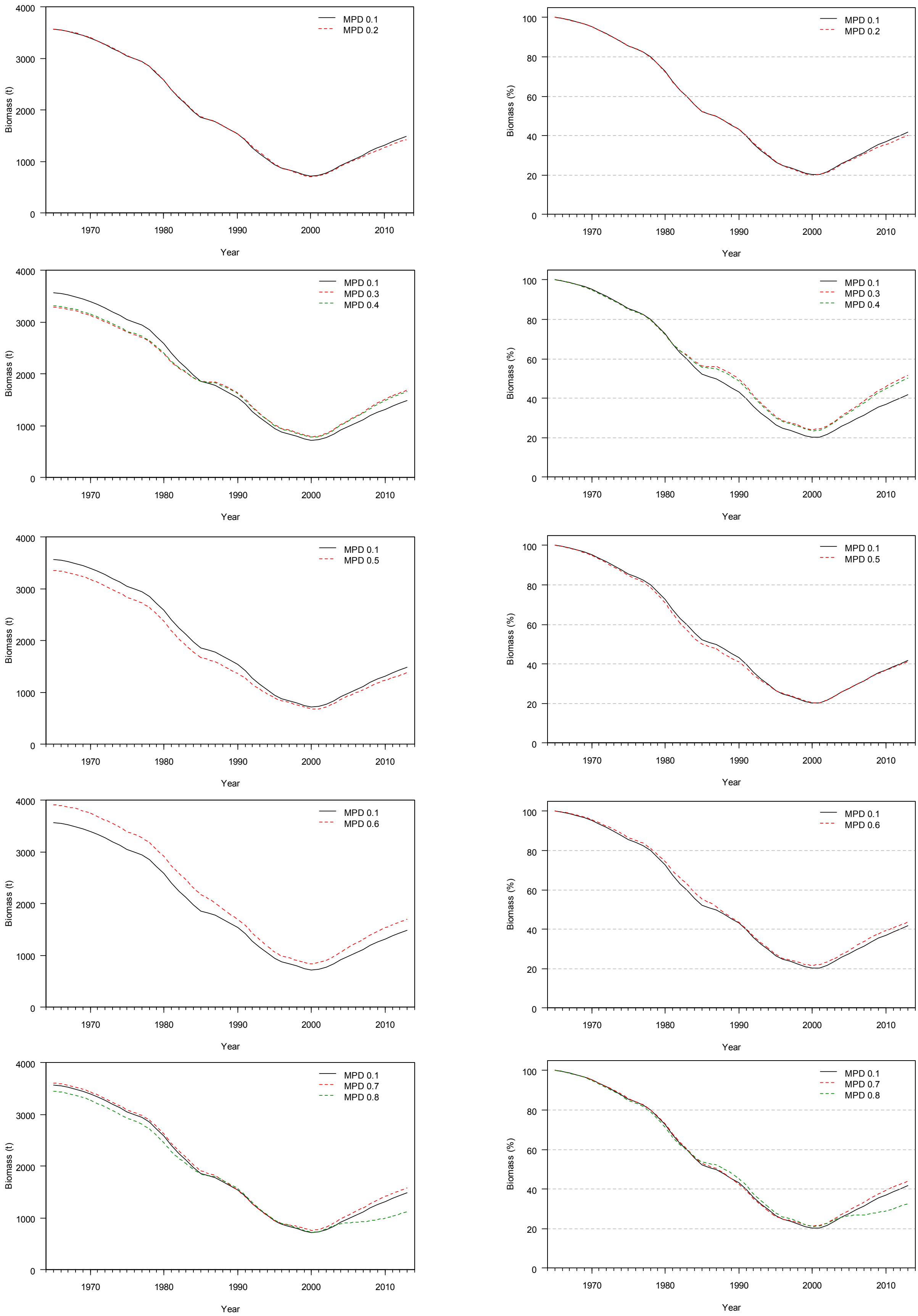

Figure 10: A comparison of Estimated spawning (left) and spawning biomass as a percentage of the virgin level (right) for MPD base case model (0.1 and selected sensitivity model runs (See

Table 4).

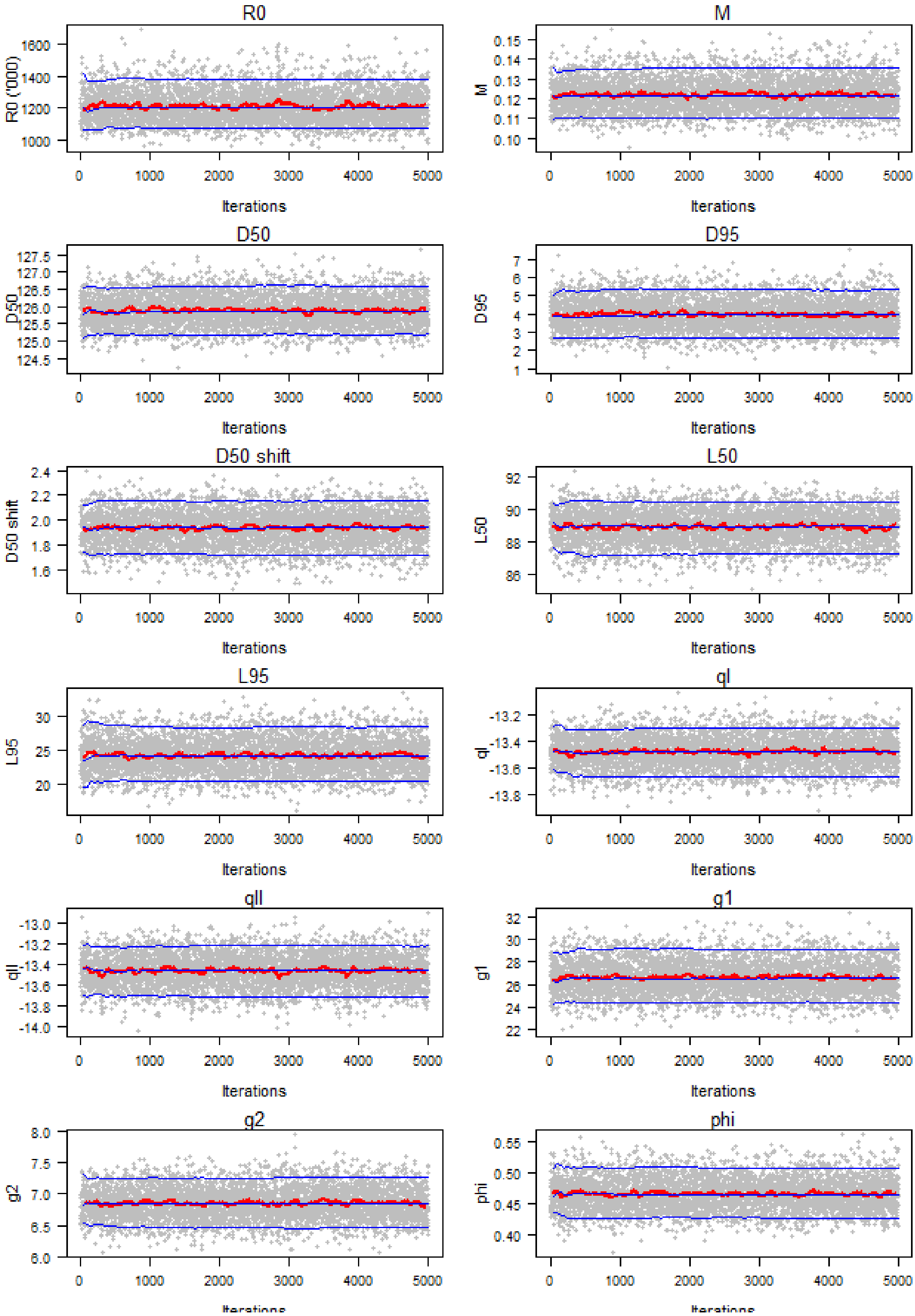

Figure 11: Traces of estimated parameters (left) and biomass indicators (right) for base case MCMC 0.1. Blues lines are running 5, 50, and 95% quantiles of the chain and red lines are the moving average of the chain.

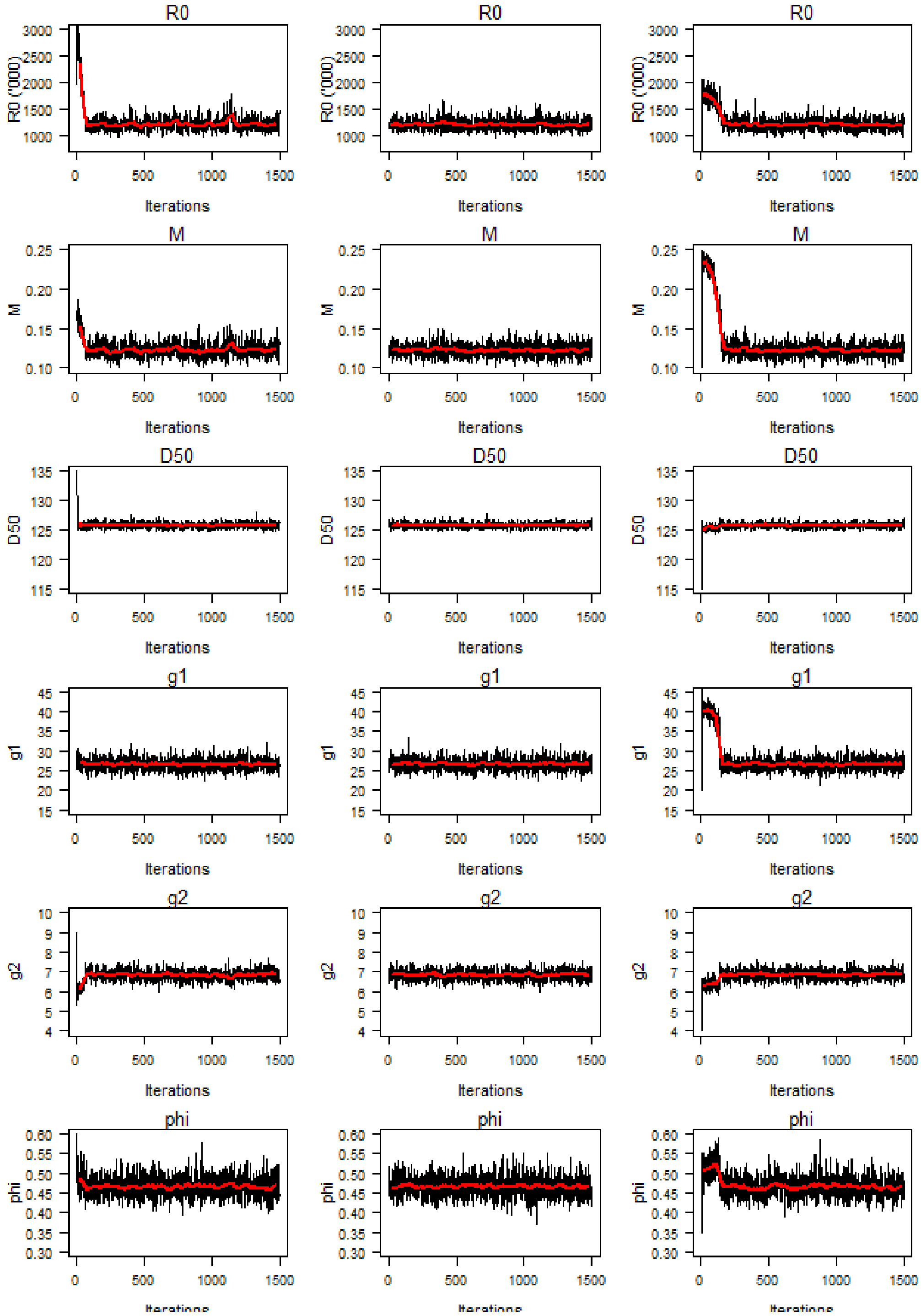

Figure 12: Traces of estimated parameters from three separate chains of different starting values for MCMC 0.1.

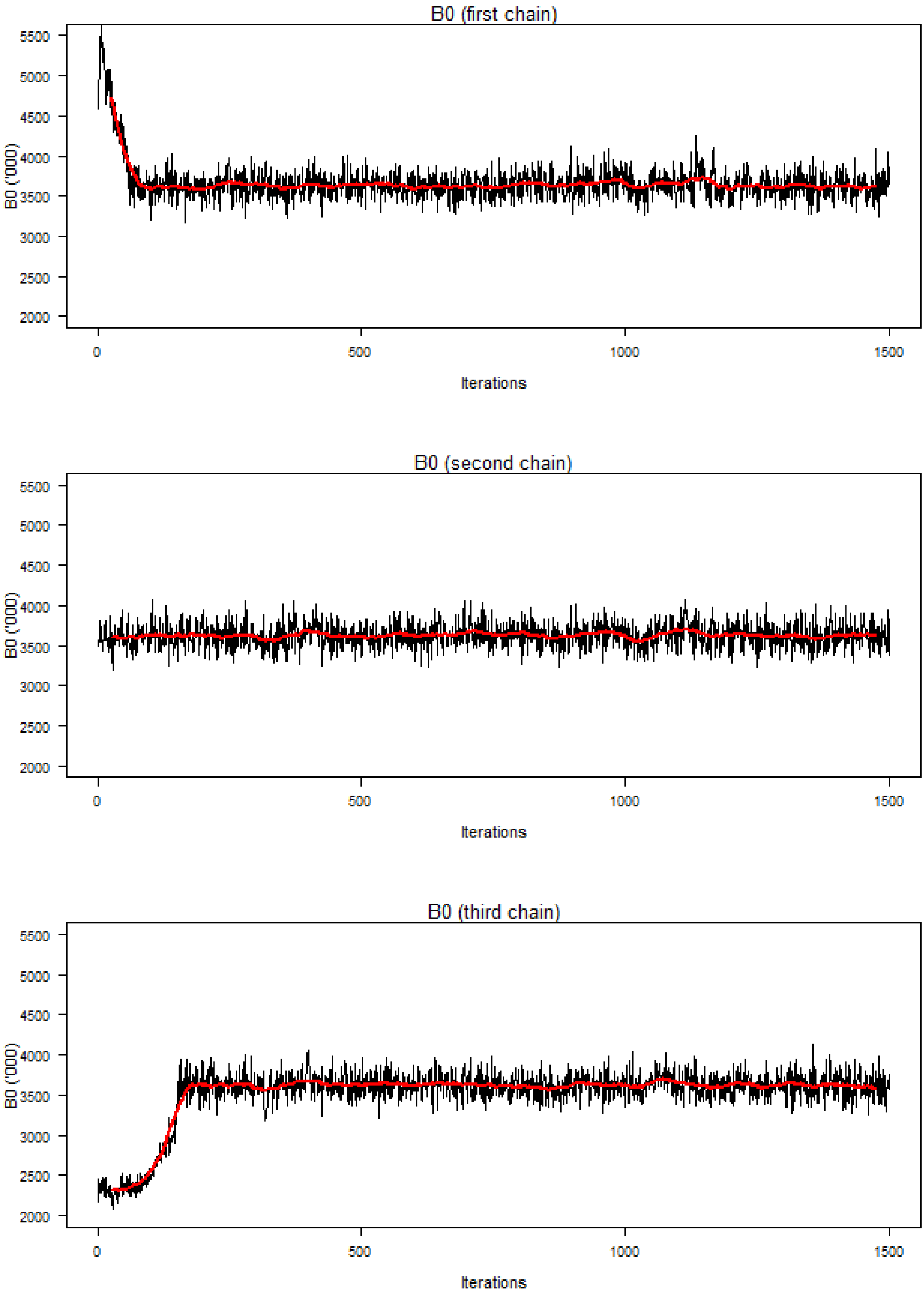

Figure 13: Traces of estimated B_0 for three MCMC runs for the base case (0.1), with parameters in each run starting from a different set of initial values.

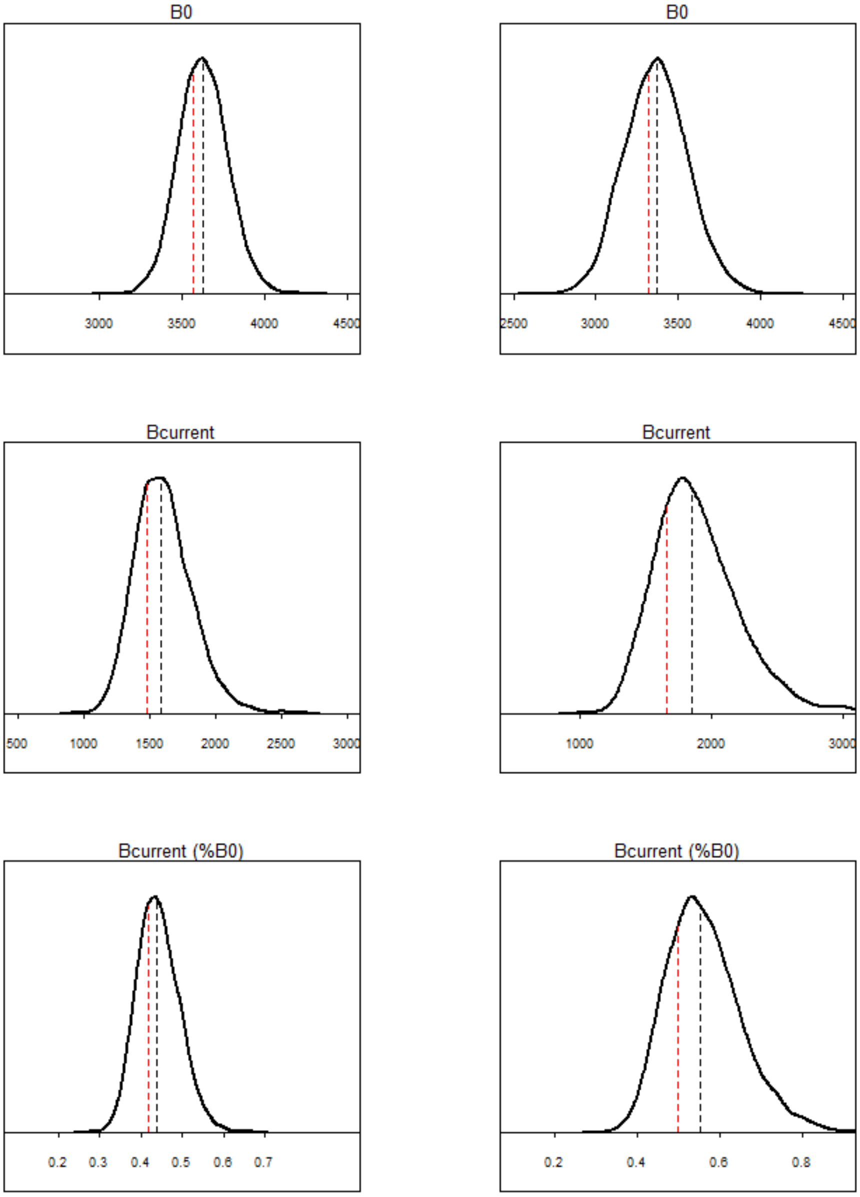

Figure 14: Posterior distribution of estimated B_0, $B_{current}$, and $B_{current}$ as a percent of B_0 for MCMC 0.1 (right) and 0.4 (right). Black dashed lines indicate median of the posterior distribution and red dashed lines indicate the MPD estimate.

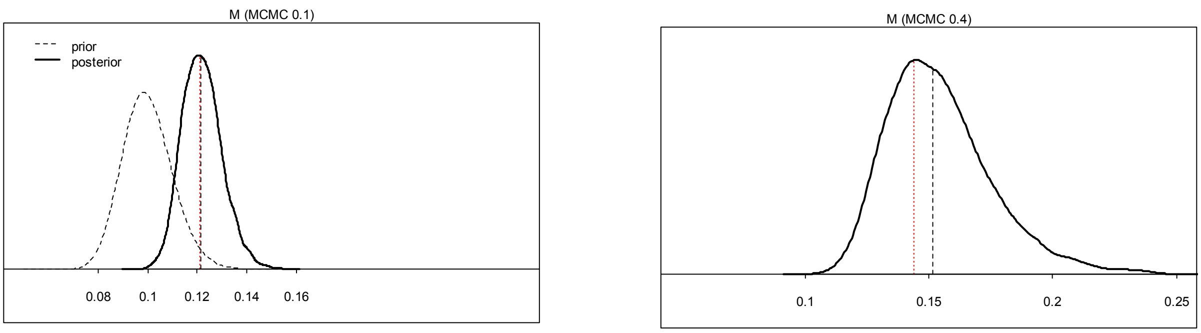

Figure 15: Posterior and prior distributions of estimated natural mortality (M) for MCMC 0.1 (right), and posterior distribution of M for MCMC 0.4 (left). The black dashed lines are the posterior median and red line and the red dashed lines are the MPD estimates.

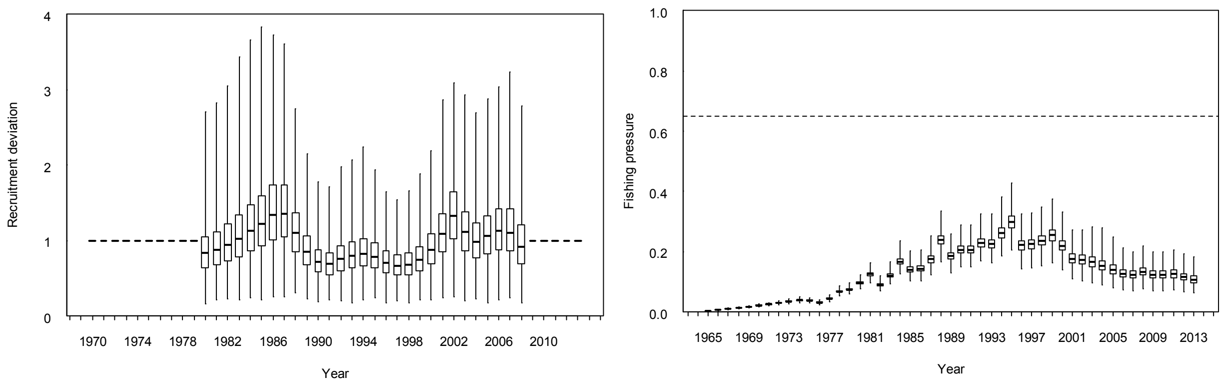

Figure 16: Posterior distributions of recruitment deviations (left), and exploitation rates (right) for MCMC 0.1. The box shows the median of the posterior distribution (horizontal bar), the 25th and 75th percentiles (box), with the whiskers representing the full range of the distribution. Recruitment deviations were estimated for 1980–2008, and fixed at 1 for other years.

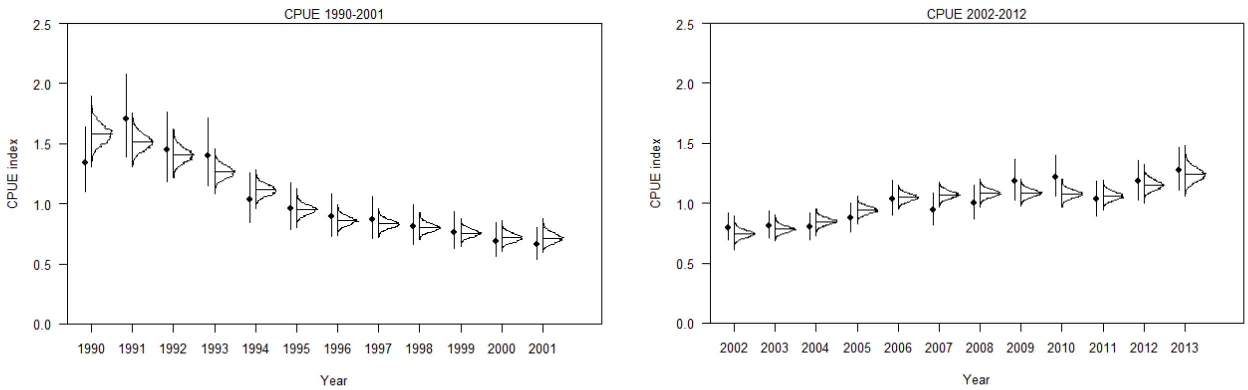

Figure 17: Posterior distributions of model predicted CPUE indices for 1990–2001 (left) and 2002–2012 (right) for MCMC 0.1 (Medians are shown as horizontal lines). Dots are observed CPUE indices and vertical lines are 95% confidence intervals.

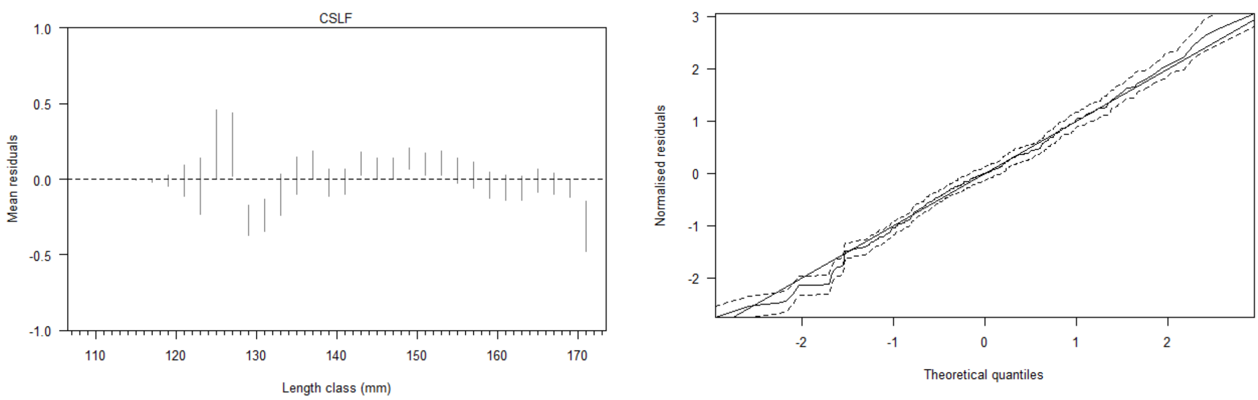

Figure 18: 95% credible intervals of the posterior distributions of mean residuals (across all years) of fits to the CSLF data (left) and the QQ quantiles of posterior distributions of residuals of fits to the tag recapture data (right).

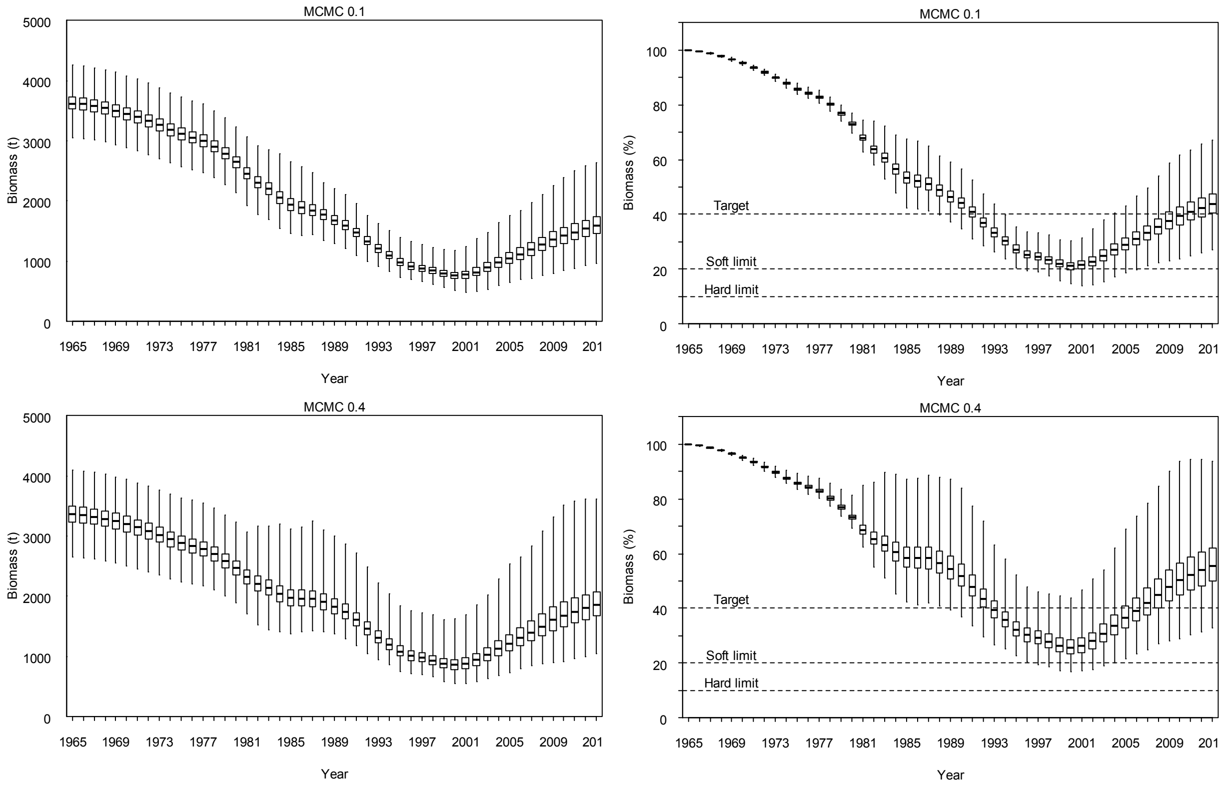

Figure 19: Posterior distributions of spawning stock biomass and spawning stock biomass as a percentage of virgin level from MCMC 0.1 and 0.4. The box shows the median of the posterior distribution (horizontal bar), the 25th and 75th percentiles (box), with the whiskers representing the full range of the distribution.

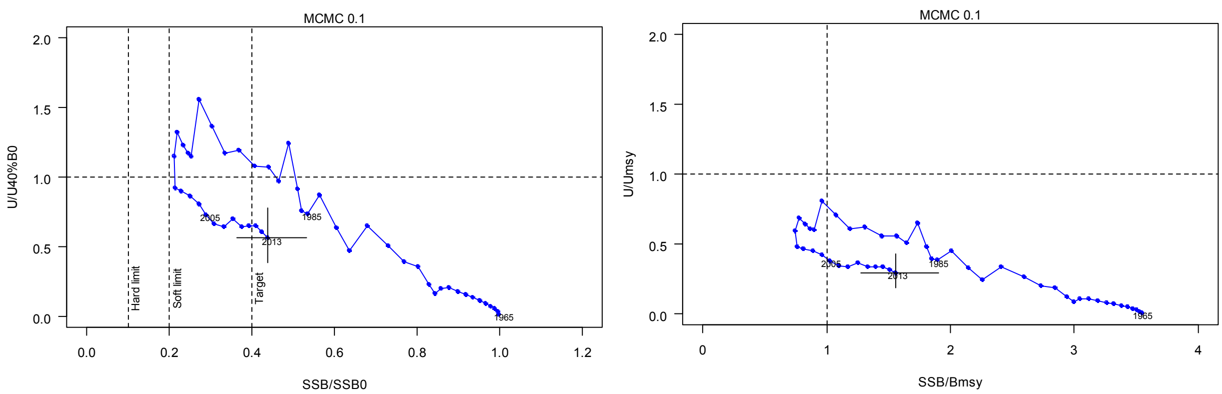

Figure 20: Trajectory of exploitation rate as a ratio of $U_{\%40B0}$ and spawning stock biomass as a ratio of B_0 (left), and exploitation rate as a ratio of U_{msy} and spawning stock biomass as a ratio of B_{msy} from the start of assessment period 1965 to 2012 for MCMC 0.1 (base case). The vertical lines at 10%, 20% and 40% B_0 represent the soft limit, the hard limit, and the target. Estimates are based on MCMC median and the 2013 90% CI is shown by the cross line.

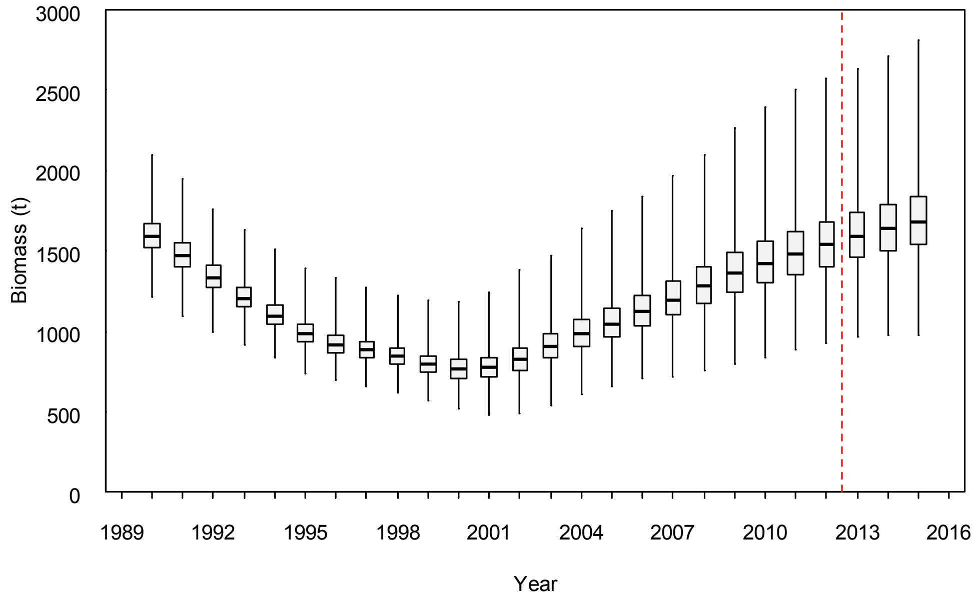

Figure 21: Posterior distributions of projected spawning stock biomass with future commercial catch set to current TACC and future minimum harvest size set to 135 mm for MCMC 0.1 (base case). The box shows the median of the posterior distribution (horizontal bar), the 25th and 75th percentiles (box), with the whiskers representing the full range of the distribution.

APPENDIX A: SUMMARY MPD MODEL FITS AND ESTIMATES

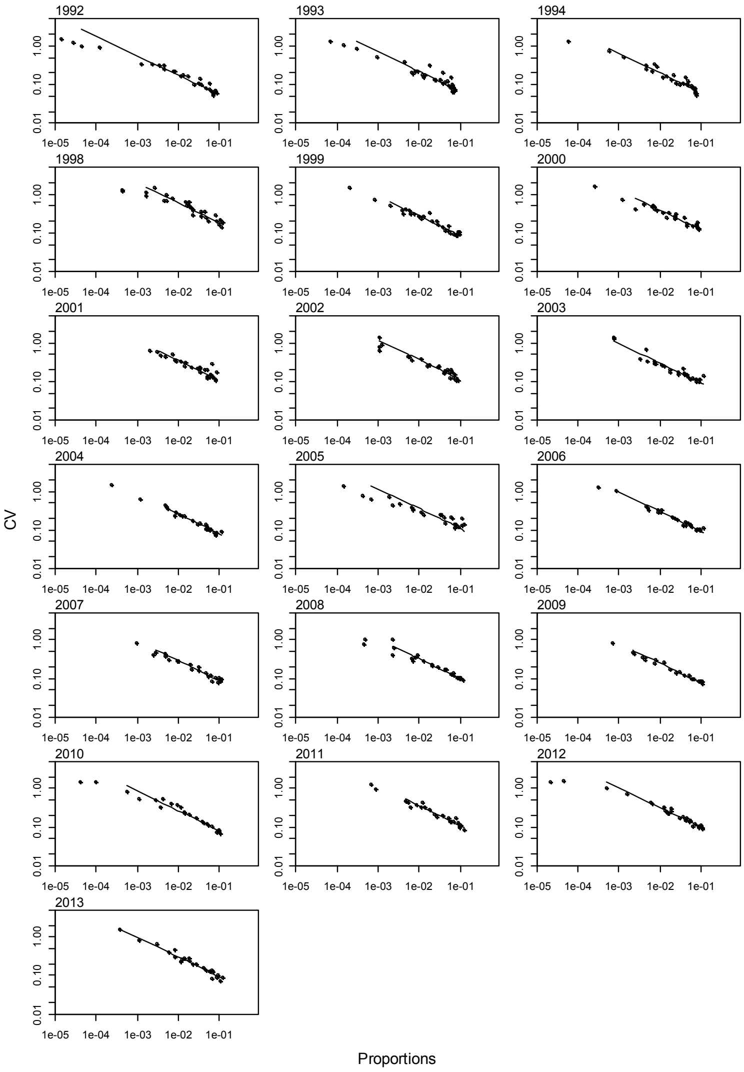

Figure A1: Estimated proportions versus CVs for the commercial catch length frequencies in PAU 5D. Lines indicate the best least squares fit for the effective sample size of the multinomial distribution. Length frequencies 1998, 2002–04, 2007, 2009–2012 were included in the assessment models.

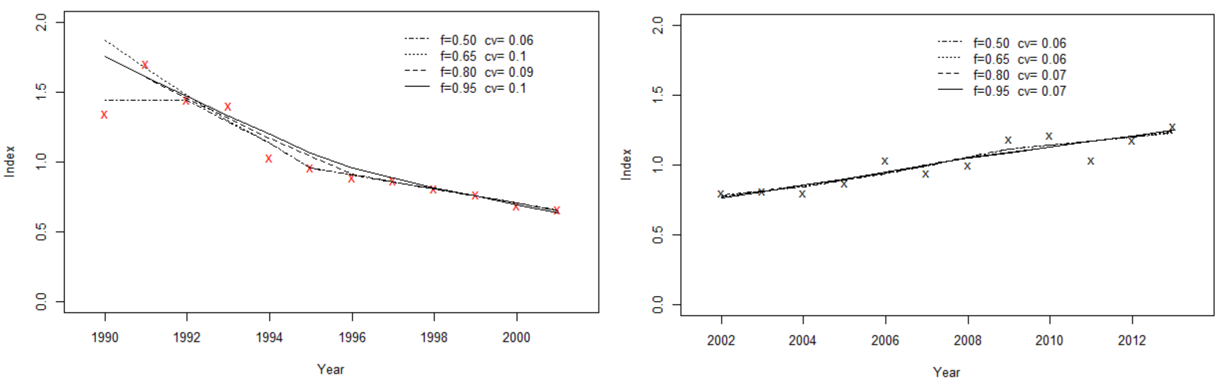

Figure A2: A series of lowess lines of various degrees of freedom (f) fitted to the PAU 5B standardised CPUE indices for 1990–2001 (left) and for 2002–2013 (right). CVs are calculated from residuals for each of the fitted lowess line. The CV of the residuals from the "appropriate" fit will be used as the CV in the stock assessment model. What is "appropriate" is judged by visual examination of lines with different degrees of smoothing. This approach is recommended by Francis (2011).

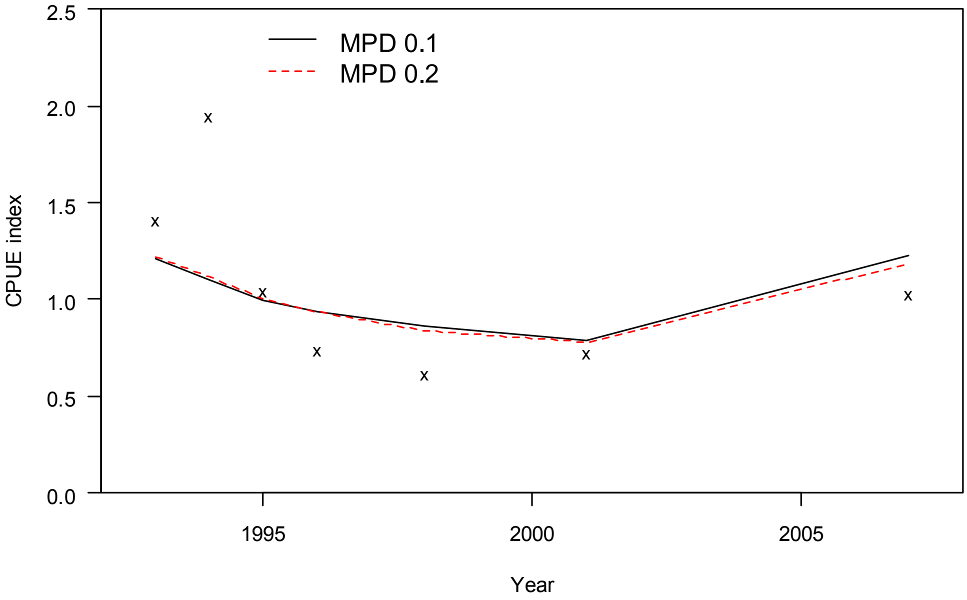

Figure A3: Comparison of fits to the RDSI for MPD 0.1 (base case) and MPD 0.2. For MPD 0.1 the RDSI was excluded from the model and the fits are model predicted values.

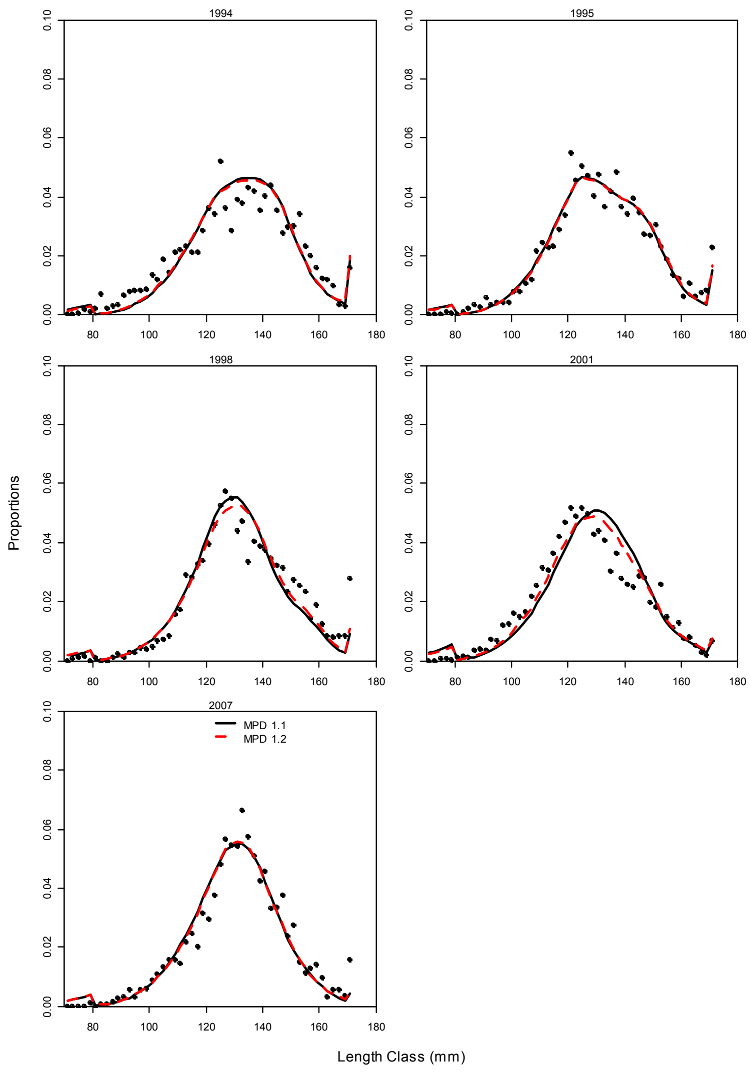

Figure A4: Comparison of fits to the RDLF for MPD 0.1 (base case) and MPD 0.2. For MPD 0.1 the RDLF was excluded from the model and the fits shown here are model predicted values.

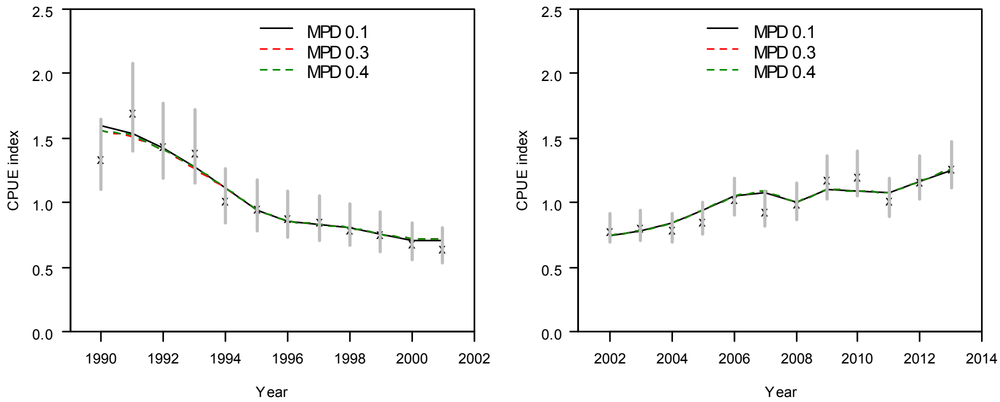

Figure A5: Comparison of fits to the CPUE and PCPUE data for MPD 0.1 (base case), MPD 0.3, and MPD 0.4.

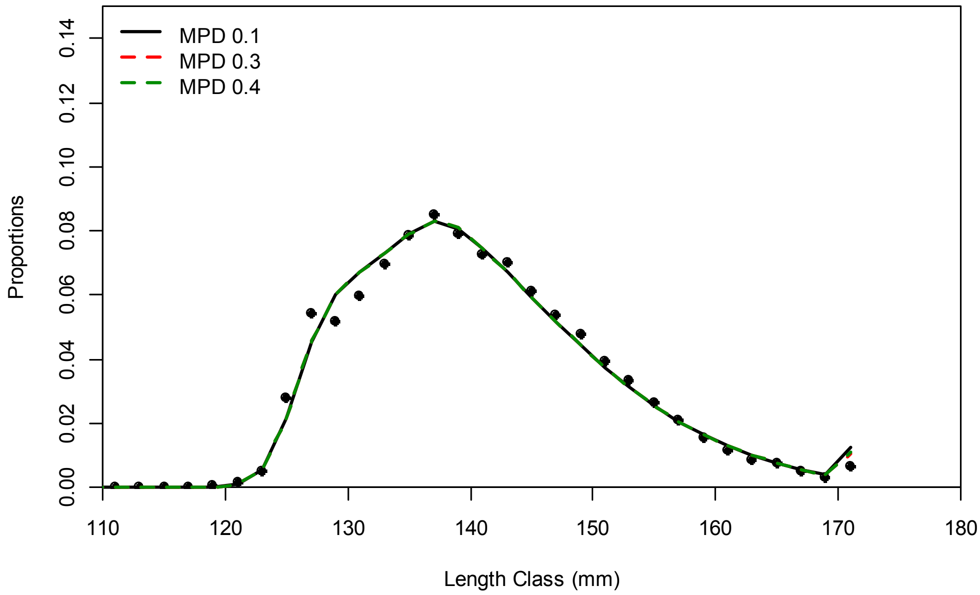

Figure A6: Comparison of fits to the CSLF data for MPD 0.1 (base case), MPD 0.3 and MPD 0.4. The fits and observations are averaged over all years.

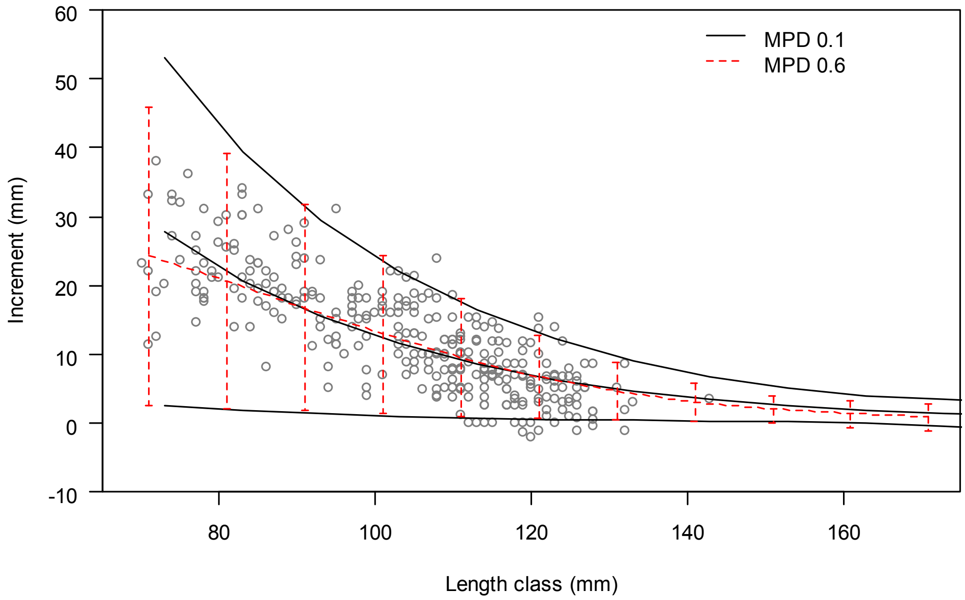

Figure A7: Comparison of fits to the growth data for MPD 0.1 (base case), MPD 0.6.

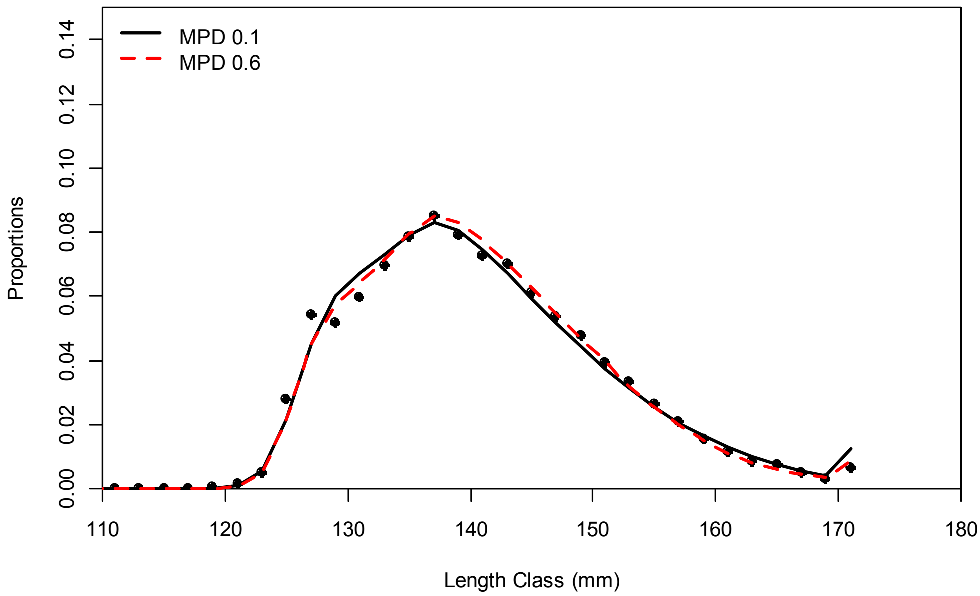

Figure A8: Comparison of fits to the CSLF data for MPD 0.1 (base case), MPD 0.6. The fits and observations are averaged over all years.